

**Exotic Structures at the Neutron
Drip Line and Stability of Neutron Matter**
In the Memory of K. A. Gridnev

D. Gridnev^{1,2}

in collaboration with

**V. N. TARASOV³, S. SCHRAMM², D. K. GRIDNEV²,
X. VIÑAS⁴ AND WALTER GREINER²**

¹ *Saint Petersburg State University, St. Petersburg, Russia;*

² *Frankfurt Institute for Advanced Studies, J.W.G. University, Frankfurt, Germany;*

³ *NSC Kharkov Institute of Physics and Technology, Kharkov, Ukraine;*

⁴ *University of Barcelona, Barcelona, Spain;*

Skyrme Forces

$$V_{ij} = t_0(1 + x_0 P_\sigma) \delta(\vec{r}) + \frac{1}{2} t_1 (1 + x_1 P_\sigma) [\vec{k}'^2 \delta(\vec{r}) + \delta(\vec{r}) \vec{k}^2] + \\ + t_2 (1 + x_2 P_\sigma) \vec{k}' \delta(\vec{r}) \vec{k} + \frac{1}{6} t_3 (1 + x_3 P_\sigma) \rho^\alpha(\vec{R}) \delta(\vec{r}) + i W_0 [\vec{k}' \times \delta(\vec{r}) \vec{k}] (\vec{\sigma}_i + \vec{\sigma}_j),$$

where $\vec{r} = \vec{r}_i - \vec{r}_j$, $\vec{R} = \frac{1}{2}(\vec{r}_i + \vec{r}_j)$, $\vec{k} = \frac{-i}{2}(\vec{\nabla}_i - \vec{\nabla}_j)$, $\vec{k}' = \frac{i}{2}(\vec{\nabla}_i - \vec{\nabla}_j)$, $P_\sigma = \frac{1}{2}(1 + \vec{\sigma}_i \cdot \vec{\sigma}_j)$,

$t_n, x_n (n = 0, 1, 2, 3), \alpha, W_0$ - parameters.

Skyrme Forces used in the calculations

Force	t_0 MeV fm ³	t_1 MeV fm ⁵	t_2 MeV fm ⁵	t_3 MeV fm ^{3+3α}	x_0	x_1	x_2	x_3	W_0 MeV fm ⁵	α
SLy4	-2488,91	486,82	-546,39	13777,0	0,834	-0,344	-1,000	1,354	123,0	1/6
SkM*	-2645.00	410.00	-135.00	15595.0	0.090	0,0	0,0	0,0	130.0	1/6
Ska	-1602,78	570,88	-67,70	8000,0	-0,020	0,0	0,0	-0,286	125,0	1/3
S3	-1128.75	395.00	-95.00	14000.0	0.450	0.0	0.0	1.0	120.0	1
SkI2	-1915.43	438.45	305.45	10548.9	-0.211	-1.738	-1.534	-0.178	120,6	1/4
SkI5	-1772.91	550.84	-126.69	8206.25	-0.117	-1.309	-1.049	0.341	123.6	1/4
SkP	-2931.70	320.62	-337.41	18709.0	0.292	0.653	-0.537	0.181	100.0	1/6

Hartree Fock Equations with Skyrme Forces

HF equations:

$$\left[-\vec{\nabla} \frac{\hbar^2}{2m_q^* (\vec{R})} \vec{\nabla} + U(\vec{R}) + \vec{\nabla} W(\vec{R}) \cdot (-i)(\vec{\nabla} \times \vec{\sigma}) \right] \Phi_i = e_i \Phi_i$$

Axially deformed oscillator basis for deformed nuclei (DHF)

$$\Phi_i(\vec{R}, \sigma, q) = \chi_{q_i}(q) \sum_{\alpha} C_{\alpha}^i \varphi_{\alpha}(\vec{R}, \sigma) \quad \varphi_{n_r, n_z, \Lambda \Sigma}(\vec{R}, \sigma) = \psi_{n_r}^{\Lambda}(r) \psi_{n_z}(z) \frac{e^{i\Lambda\varphi}}{\sqrt{2\pi}} \chi_{\Sigma}(\sigma)$$

$$\psi_{n_z}(z) = N_{n_z} \beta_z^{1/2} e^{-\xi^2/2} H_{n_z}(\xi) \quad \xi = z \beta_z \quad N_{n_z} = \left(\frac{1}{\sqrt{\pi} 2^{n_z} n_z!} \right)^{1/2}$$

$$\psi_{n_r}^{\Lambda}(r) = N_{n_r}^{\Lambda} \beta_{\perp} \sqrt{2\eta}^{1/2} e^{-\eta/2} L_{n_r}^{\Lambda}(\eta) \quad \eta = r^2 \beta_{\perp}^2 \quad N_{n_r}^{\Lambda} = \left(\frac{n_r!}{(n_r + \Lambda)!} \right)^{1/2}$$

Spherically symmetric nuclei are also solved through iterated differential equations (SHF)

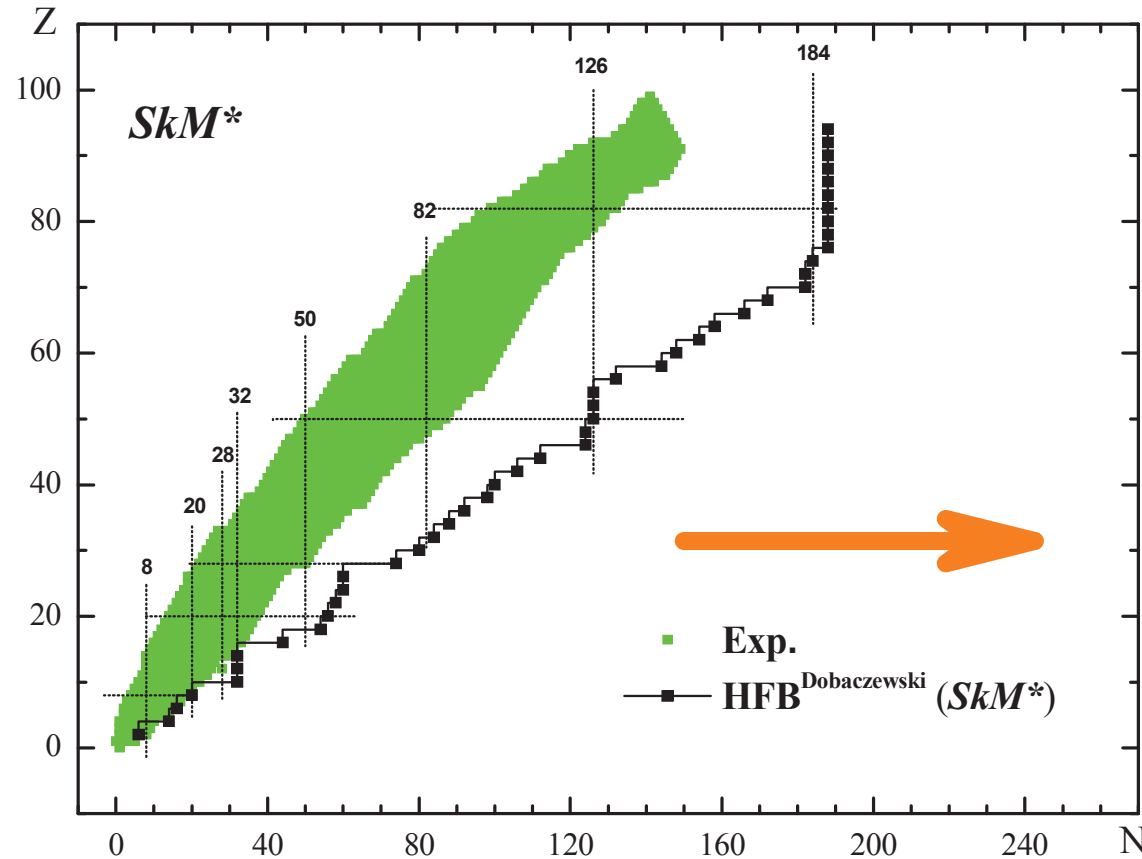
$$\frac{\hbar^2}{2m_q^*} \left[-R_{\alpha}''(r) + \frac{l_{\alpha}(l_{\alpha} + 1)}{r^2} R_{\alpha}(r) \right] - \frac{d}{dr} \left(\frac{\hbar^2}{2m_q^*} \right) R_{\alpha}'(r) + \{ U_q(r) + \frac{1}{r} \frac{d}{dr} \left(\frac{\hbar^2}{2m_q^*} \right) + [j_{\alpha}(j_{\alpha} + 1) - l_{\alpha}(l_{\alpha} + 1) - \frac{3}{4}] \times \frac{1}{r} W_q(r) \} R_{\alpha}(r) = e_{\alpha} R_{\alpha}(r)$$

BCS approximation with the pairing constant $G_{n,p} = (19.5/2)[1 \pm 0.51(N - Z)/A]$

•**DHF:** only with bound single-particle states.

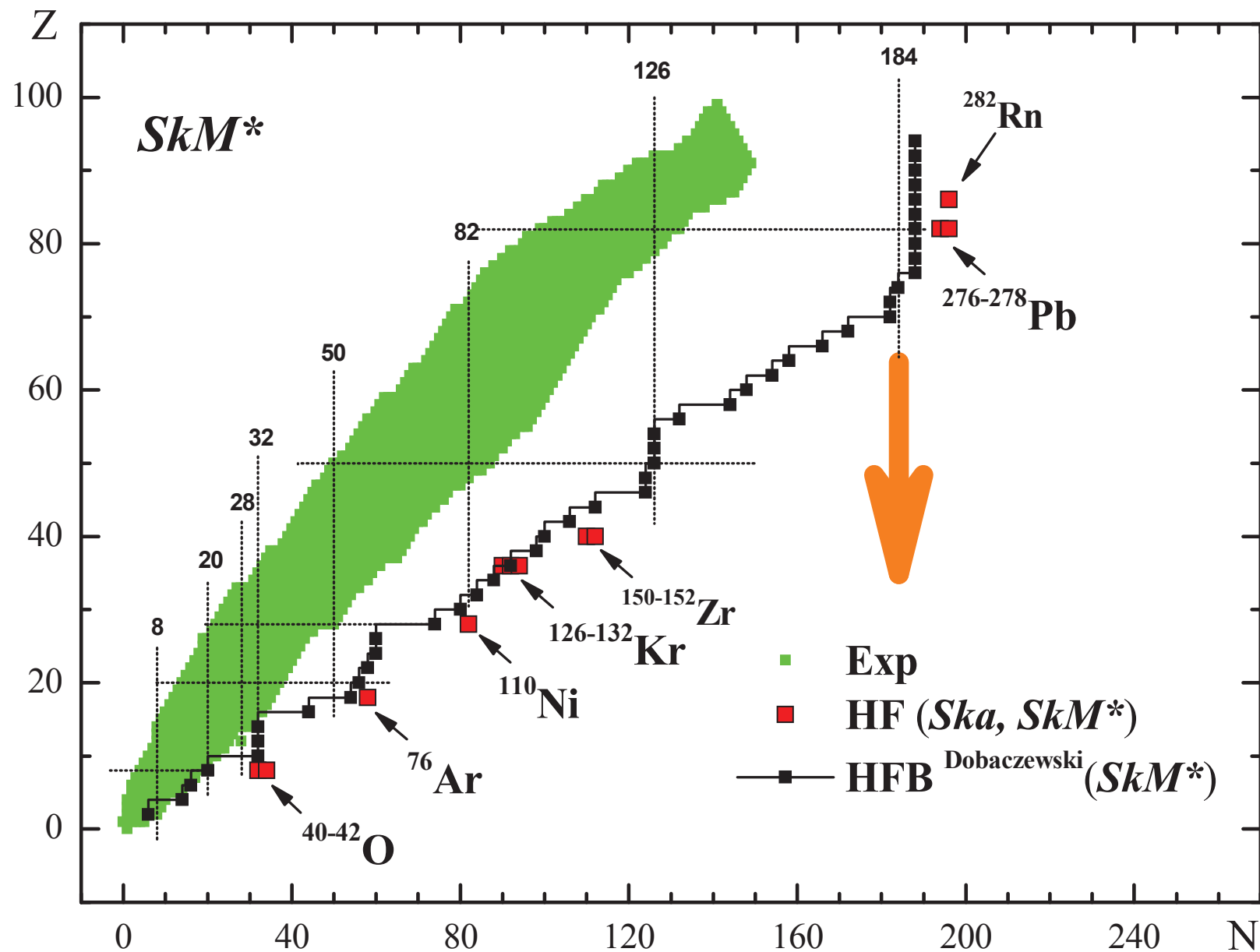
•**SHF:** also quasistable continuum states under the centrifugal barrier are included.

Nuclear Chart (HFB vs Experiment)



Green region shows the atomic nuclei which are experimentally known [Audi, Wapstra].

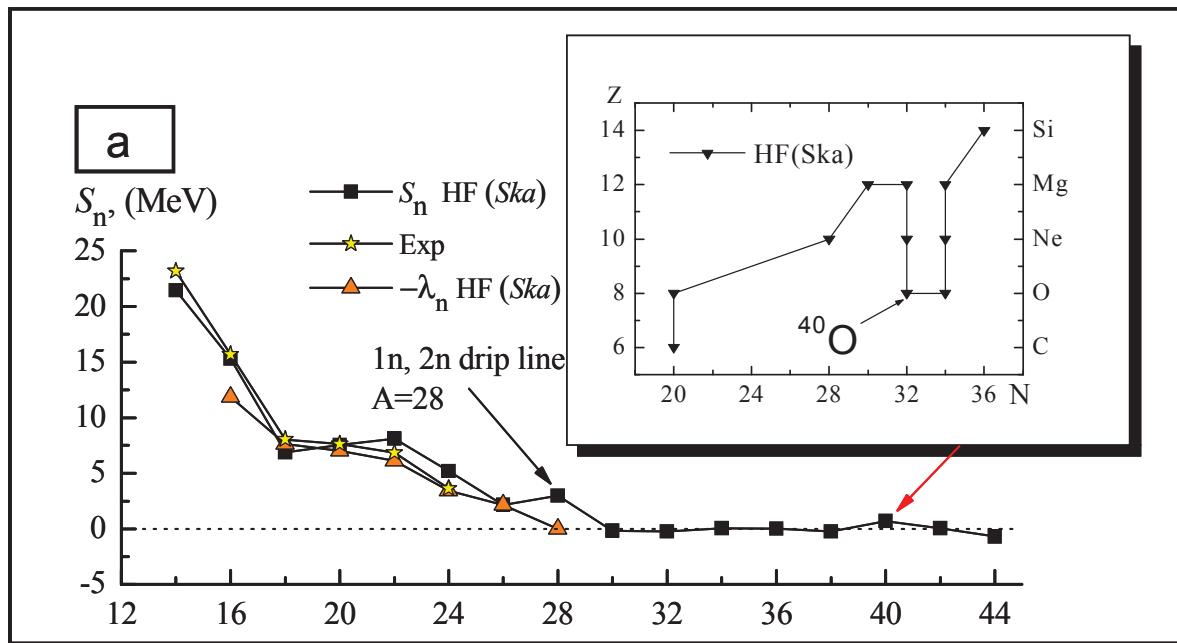
Solid line and black squares represent 1n drip line ($\lambda_n=0$) obtained in the HFB calculations with Skyrme forces SkM [Stoitsov, Dobaczewski, Nazarewicz, Pittel, PR. C68 (2003) 054312]. The orange arrow shows typical direction in the HF or HFB calculations.*



Red squares show isotopes stable with respect to one-neutron emission.

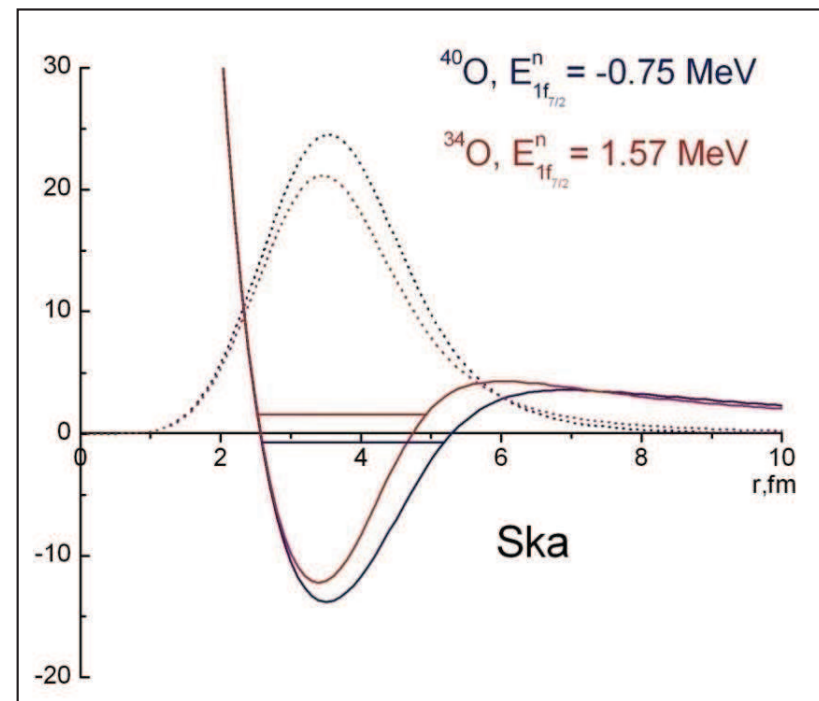
Z is changed in the direction shown by the orange arrow.

Stability enhancement should be checked on neutron magic numbers.



**One neutron
separation energies
for Oxygen and the
drip line fragment**

**The stability enhancement
through adding neutrons. The
last neutron is also confined
by the centrifugal barrier
(dotted line shows its density
distribution).**



Comparison of single particle spectra in SHF, DHF and RMF methods. Ska forces for HF and G1,2,3 and NL3 for the RMF method

Spherical with Ska		Axially deformed with Ska	
$i = nlj$	E_i	$i = \Omega^\pi$	E_i
$1s_{1/2}$	40.63	$1/2^+$	40.62
$1p_{3/2}$	25.51	$1/2^-$	25.45
		$3/2^-$	25.45
$1p_{1/2}$	21.86	$1/2^-$	21.76
$1d_{5/2}$	12.08	$3/2^+$	12.08
		$1/2^+$	12.08
		$5/2^+$	12.08
$2s_{1/2}$	9.32	$1/2^+$	9.44
$1d_{3/2}$	6.37	$3/2^+$	6.35
		$1/2^+$	6.35
$1f_{7/2}$	0.76	$5/2^-$	0.77
		$7/2^-$	0.77
		$3/2^-$	0.77
		$1/2^-$	0.77
$2p_{3/2}$	0.70	$3/2^-$	0.69
		$1/2^-$	0.69

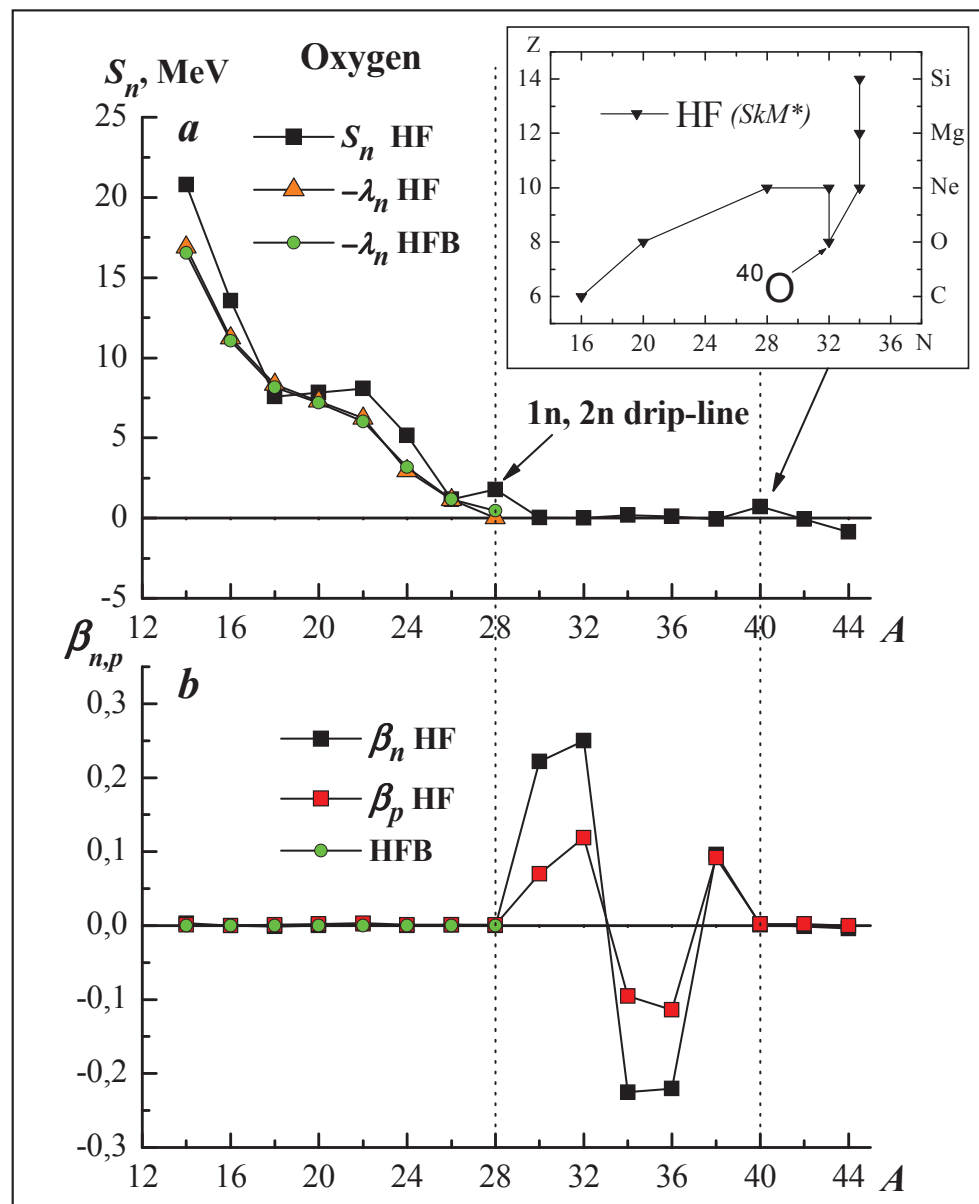
Xavier Vinyes

RMF
 ^{40}O

	G2	G1	NL3
$2p_{3/2}$	-0.958	-1.169	-1.200
$2p_{1/2}$	-	-0.505	-
$1f_{7/2}$	-0.094	0.040*	0.382

^{42}O

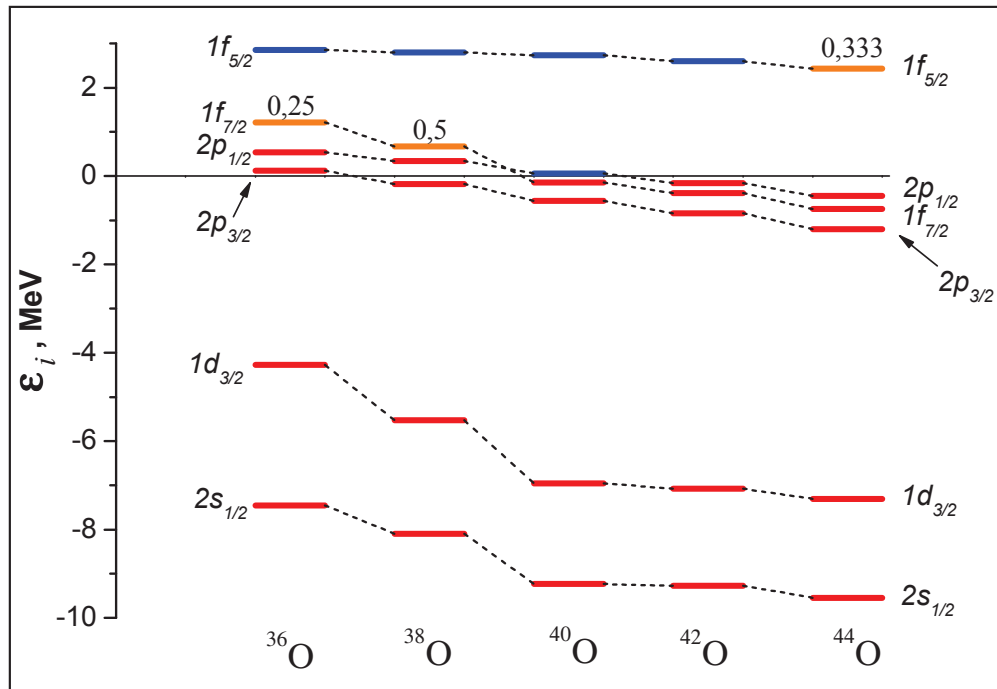
	G2	G1	NL3
$2p_{3/2}$	-1.247	-1.533	-1.495
$2p_{1/2}$	-0.562	-0.793	-0.849
$1f_{7/2}$	-0.360	-0.550	0.071



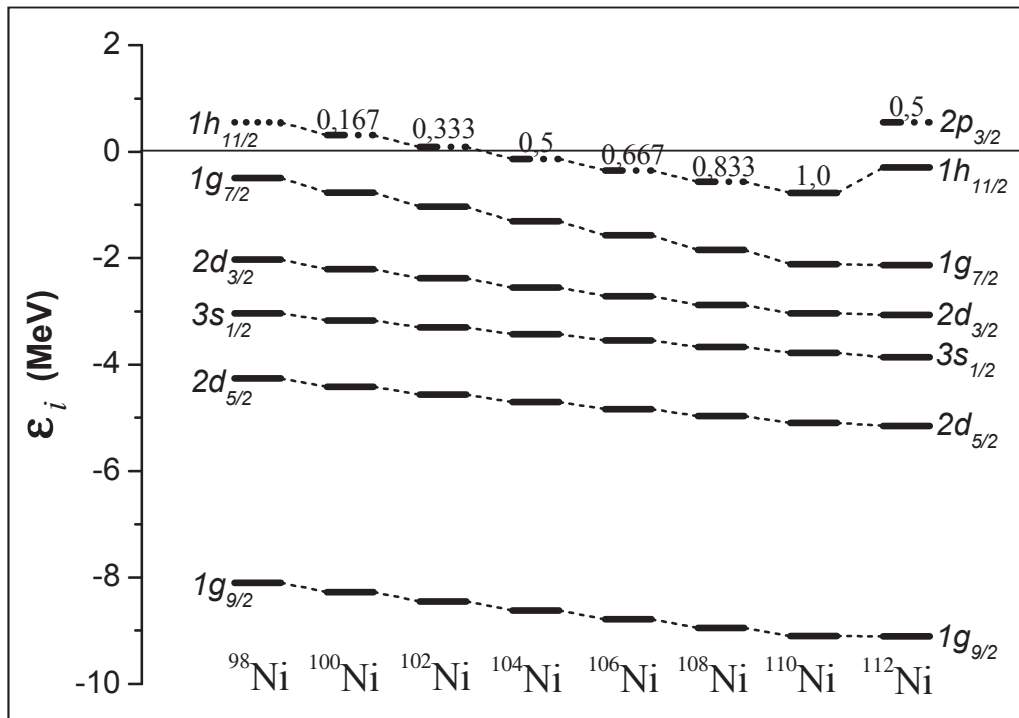
The properties of oxygen isotopes in DHF and HFB methods with SkM^ forces. The insertion represents the DHF neutron drip line.*

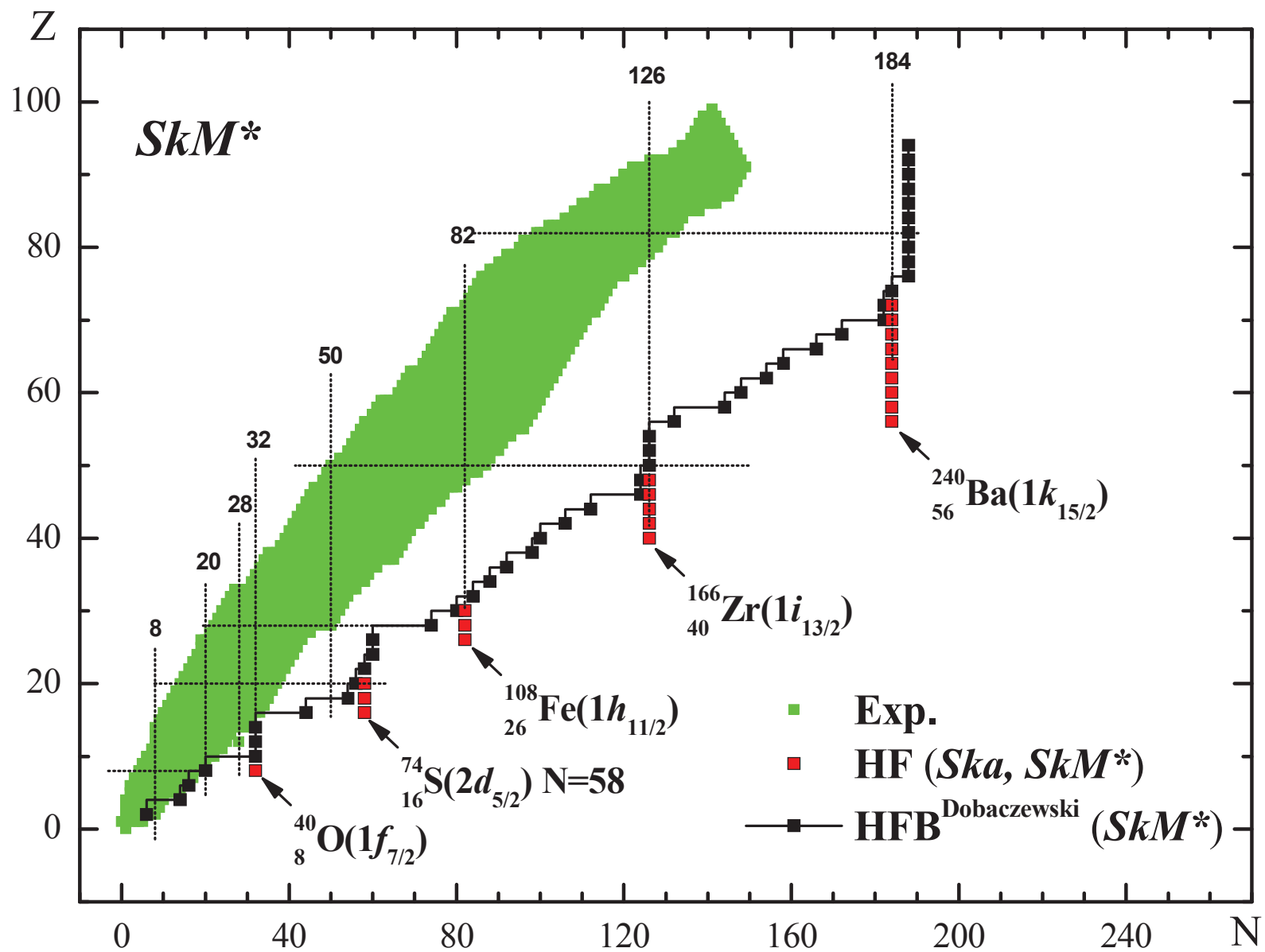
(a) - One neutron separation energies S_n and neutron chemical potential.

(b) - Neutron and proton parameters of deformation $\beta_{n,p}$.

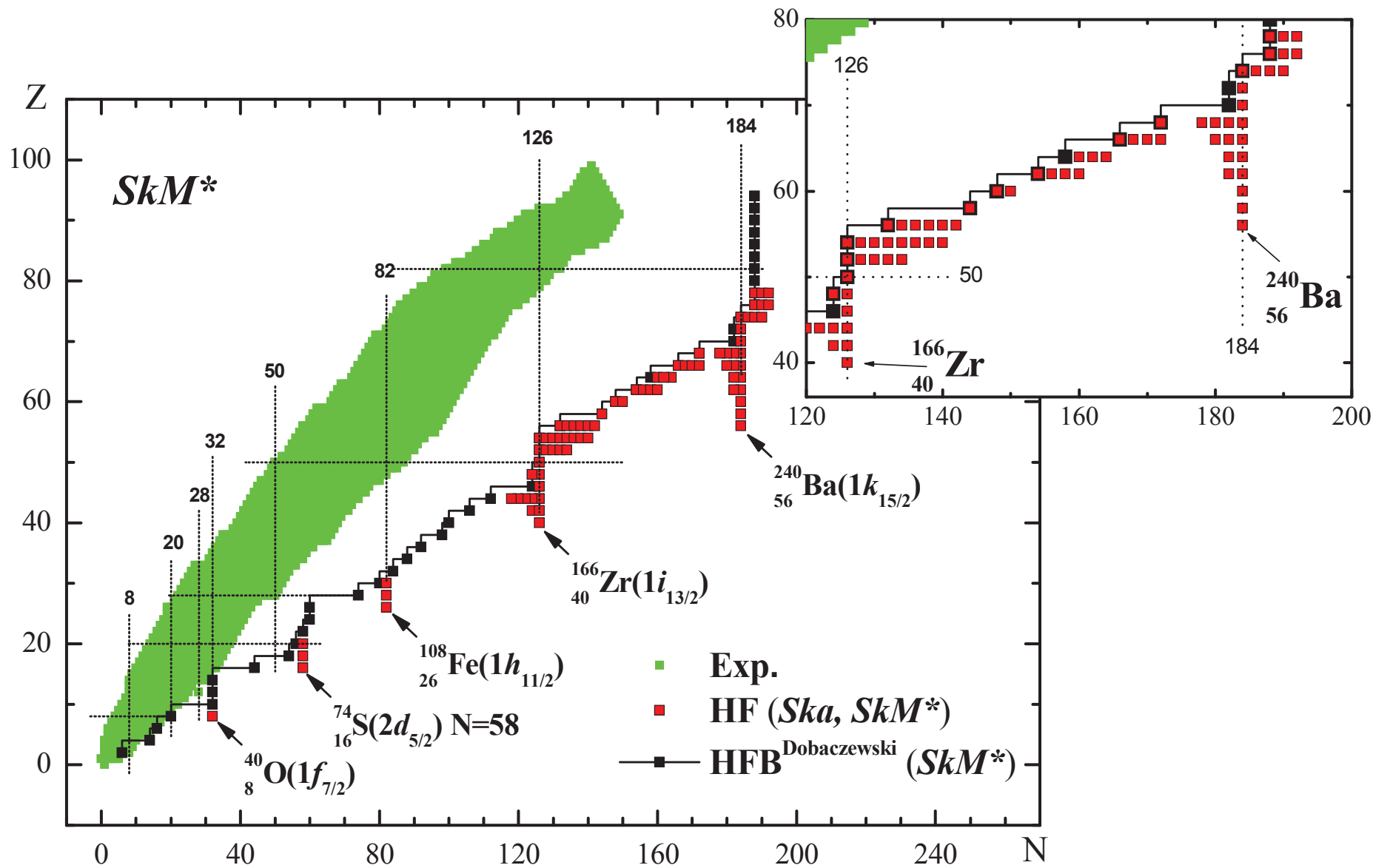


The fragments of neutron single-particle spectra for extremely neutron rich isotopes of Oxygen and Nickel.

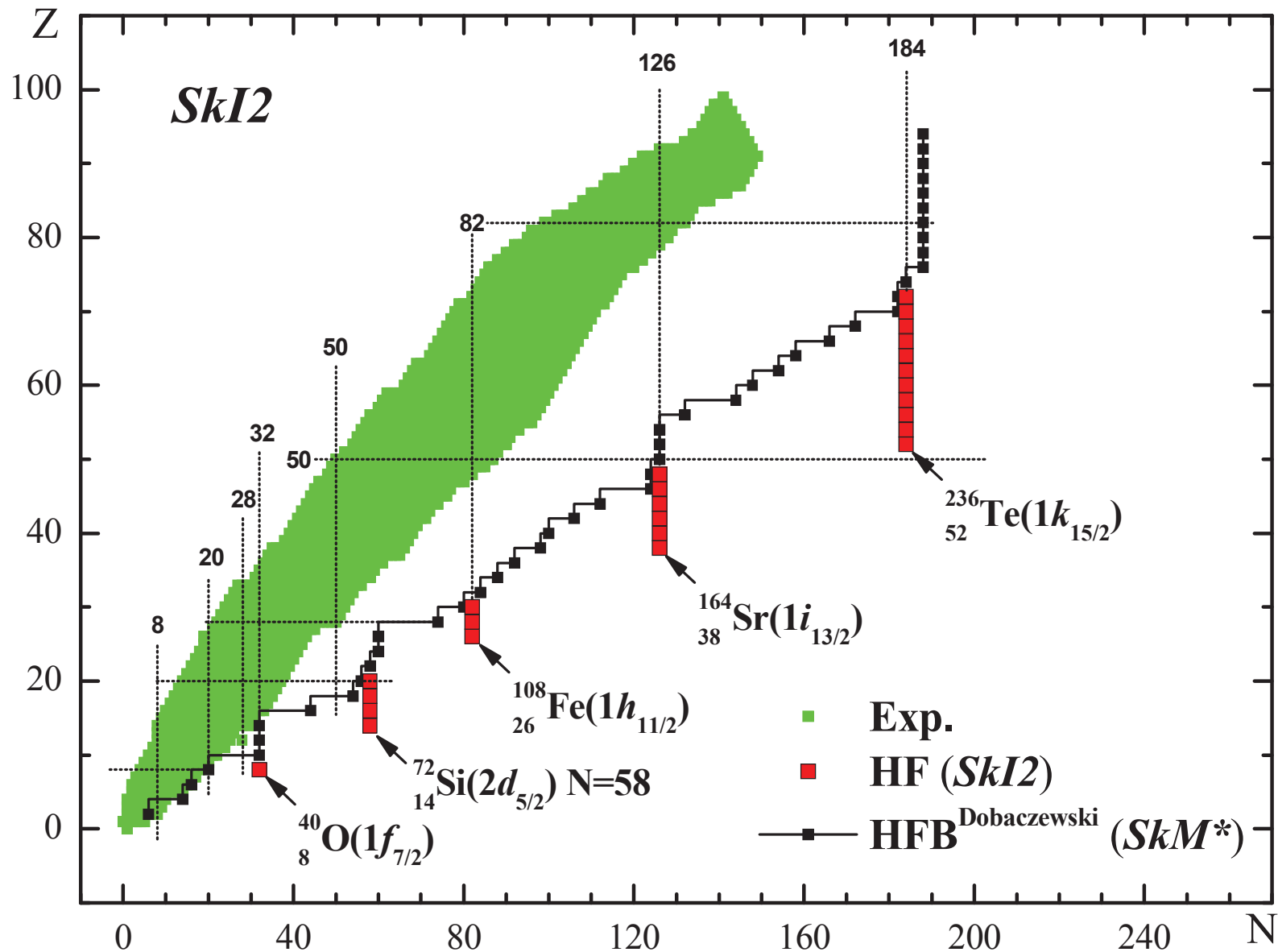




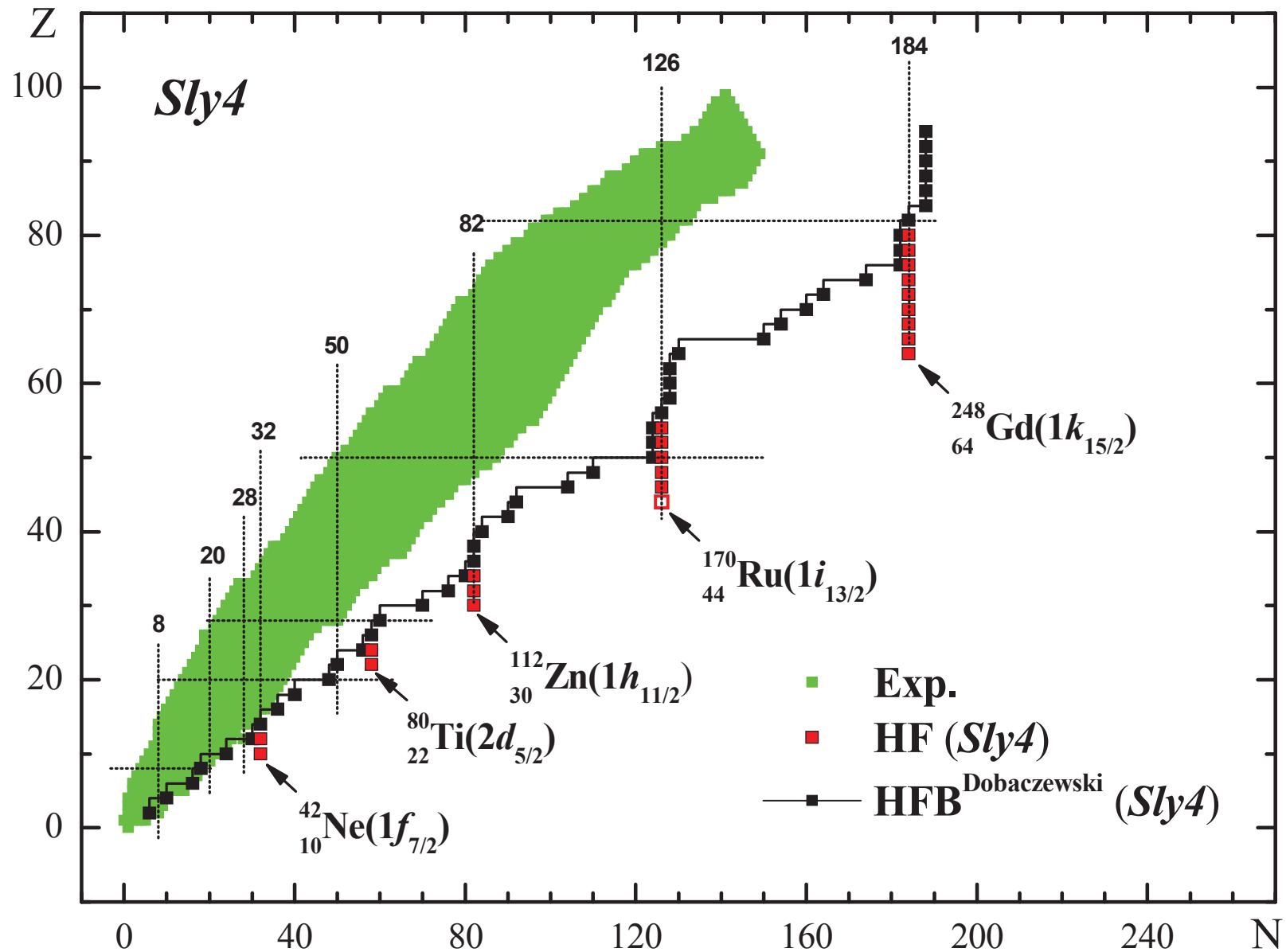
*Red squares form the peninsulas of stability.
 In brackets: the quantum numbers of the stabilizing level.*



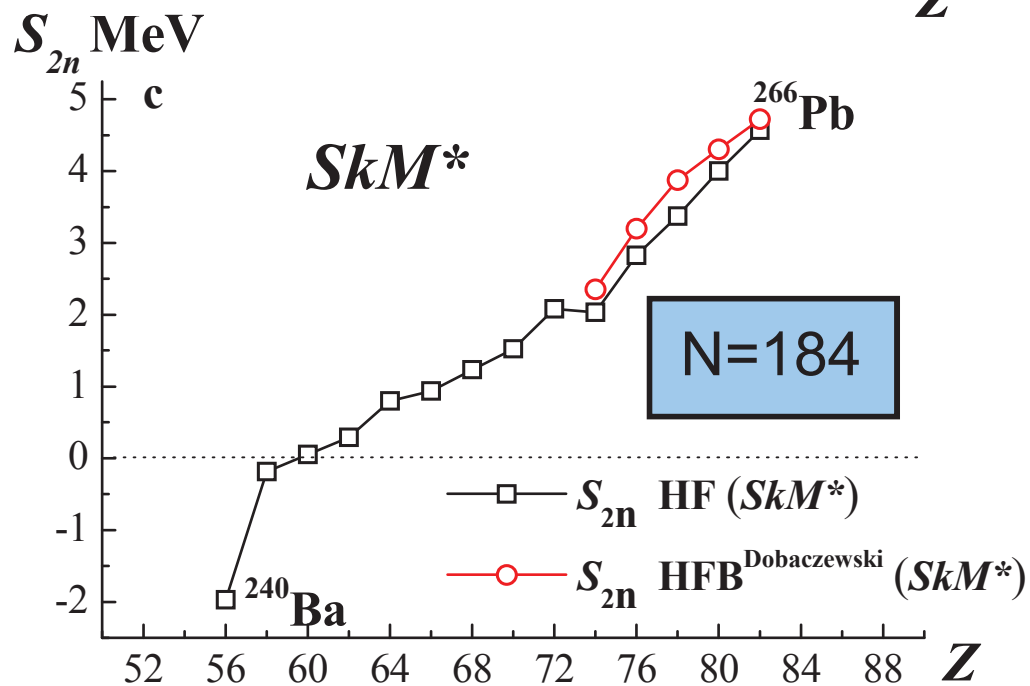
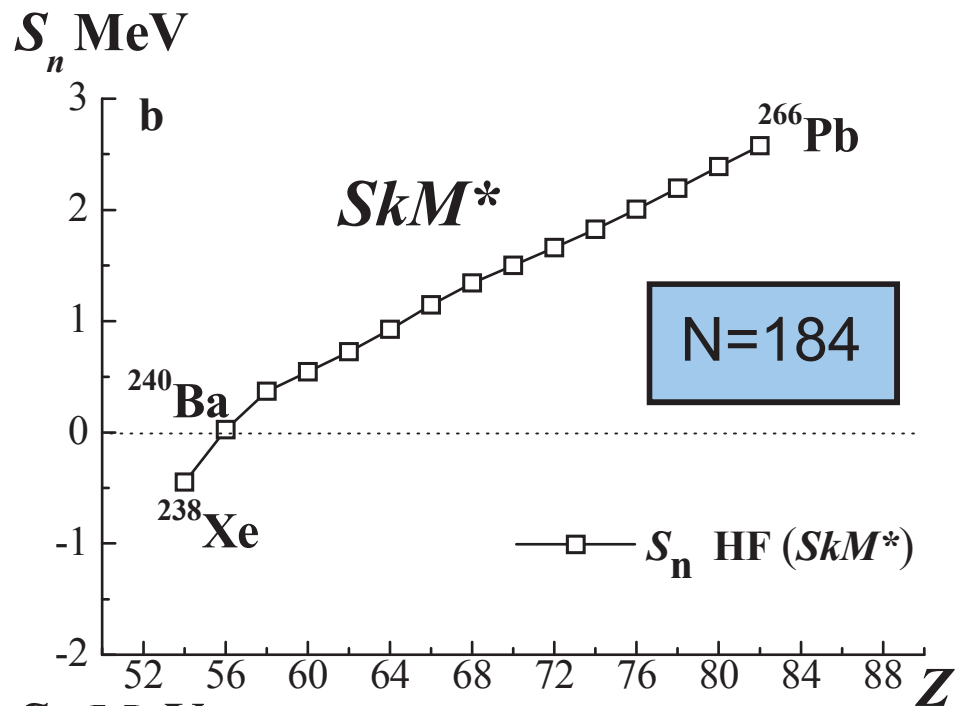
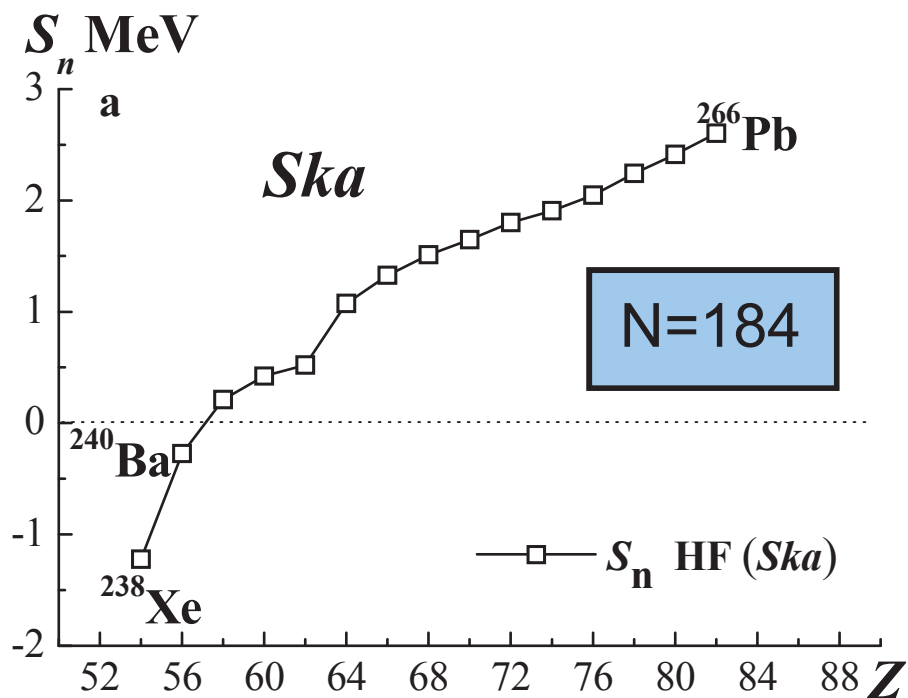
Detailed picture of stable isotopes with respect to one neutron emission between $N=126$ and $N=184$.



The same as in the previous figures but for $SkI2$ forces. The location of the peninsulas is the same, but for $N=58, 126, 184$ the peninsulas' edges appear at larger Z then for SkM^ forces. For $N=184$ the peninsula edge corresponds to Tellurium with $A=236$.*

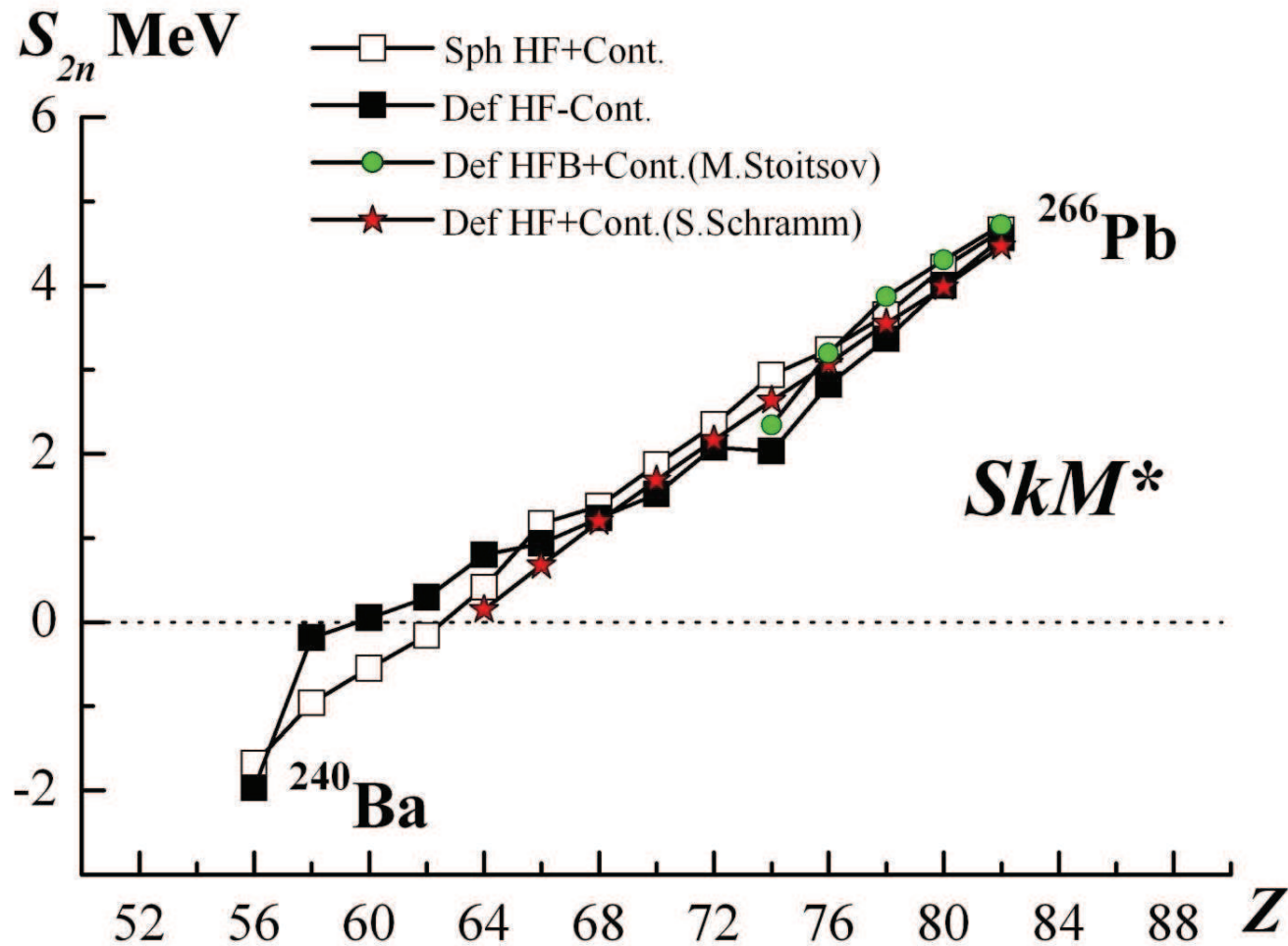


*The same as in the previous figures but for Sly4 forces.
 The location of the peninsulas is the same
 but the edges locate at smaller Z compared to SkM* and SkI2 forces.*

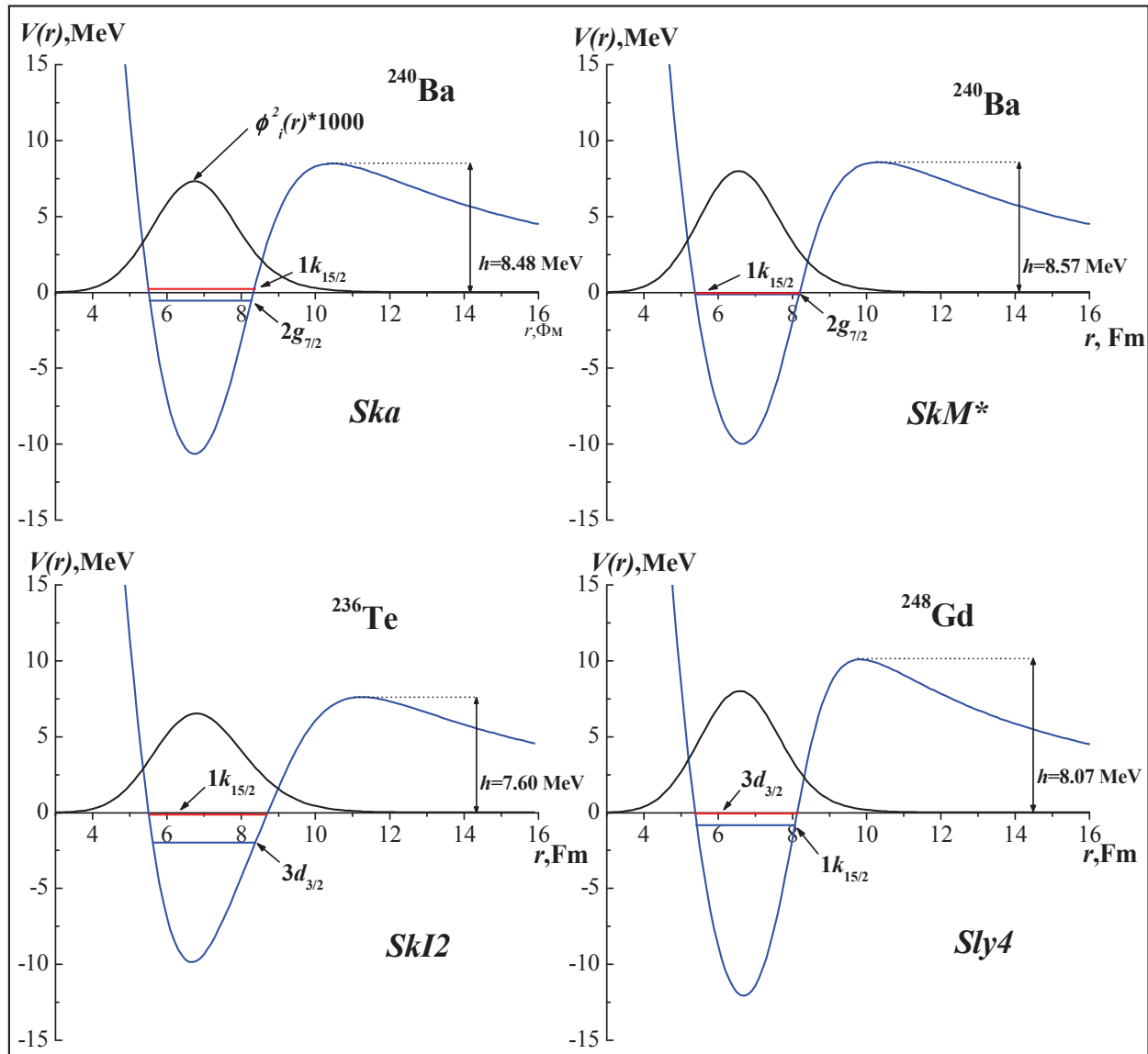


Dependences of one-neutron separation energies S_n and two-neutrons separation energies S_{2n} for the isotones with $N=184$ for the *Ska*, *SkM** forces on Z . The red line shows the S_{2n} obtained by the HFB method [PR. C68 (2003) 054312].

Comparison with grid calculations

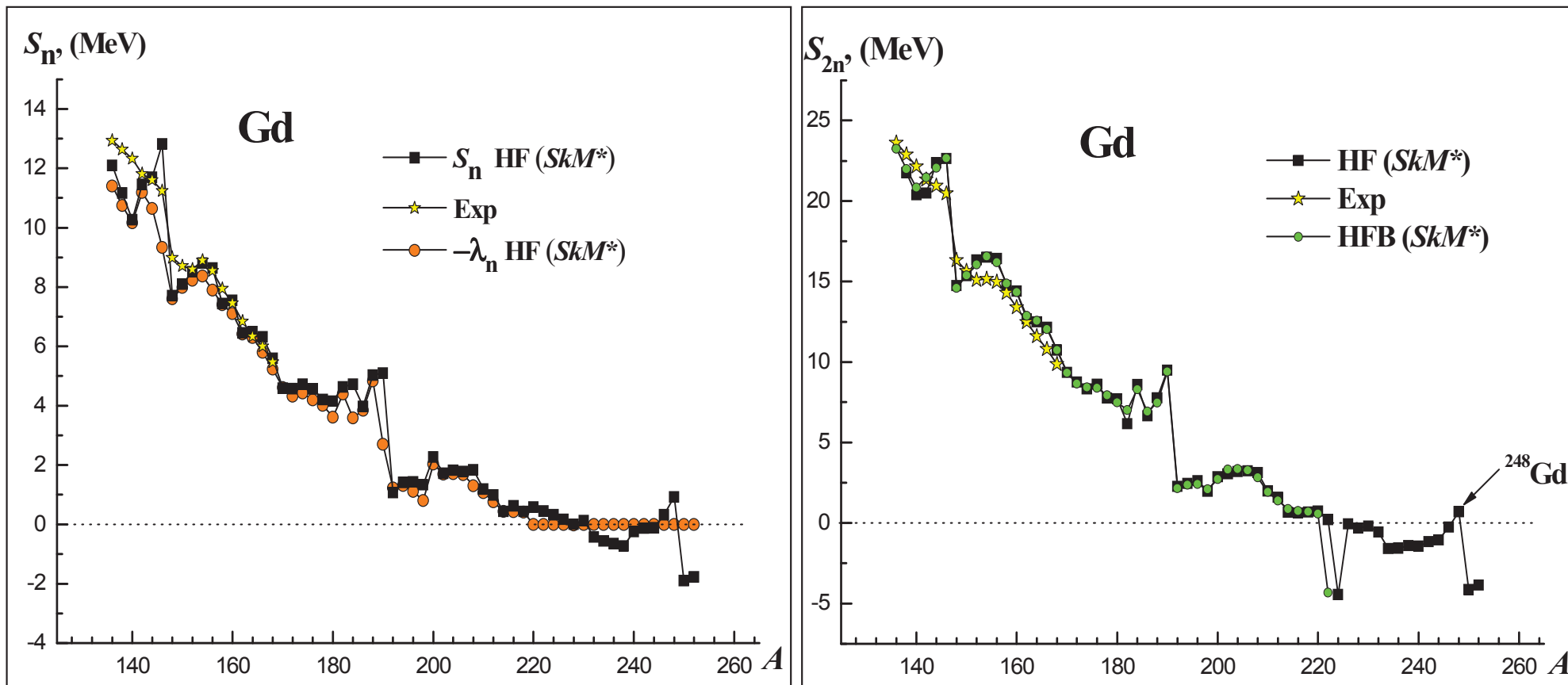


- *Empty squares: spherical equations with resonances included in BCS*
- *Black filled squares: Deformed HF with only bound states in BCS*



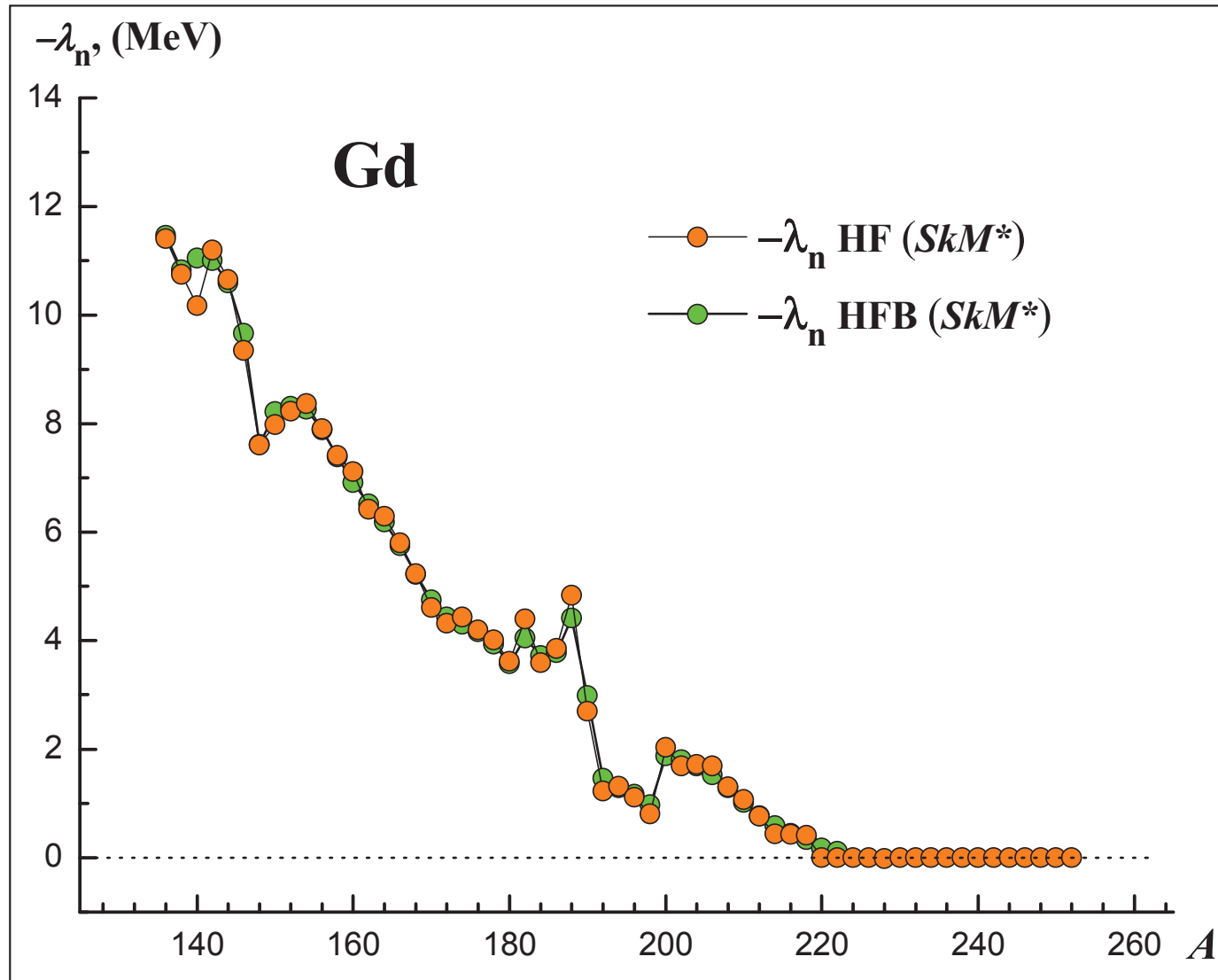
HF potentials of the last filled level of the isotones with $N=184$. Red lines show the last filled level.

The mechanism of stability enhancement at $N=184$ (the edge of stability peninsula). The appearance of peninsulas beyond the drip line is due to the complete filling of the corresponding neutron subshells with large values of angular momentum. Being partially filled these shells locate in the continuum but descend into the discrete spectrum getting further filled.

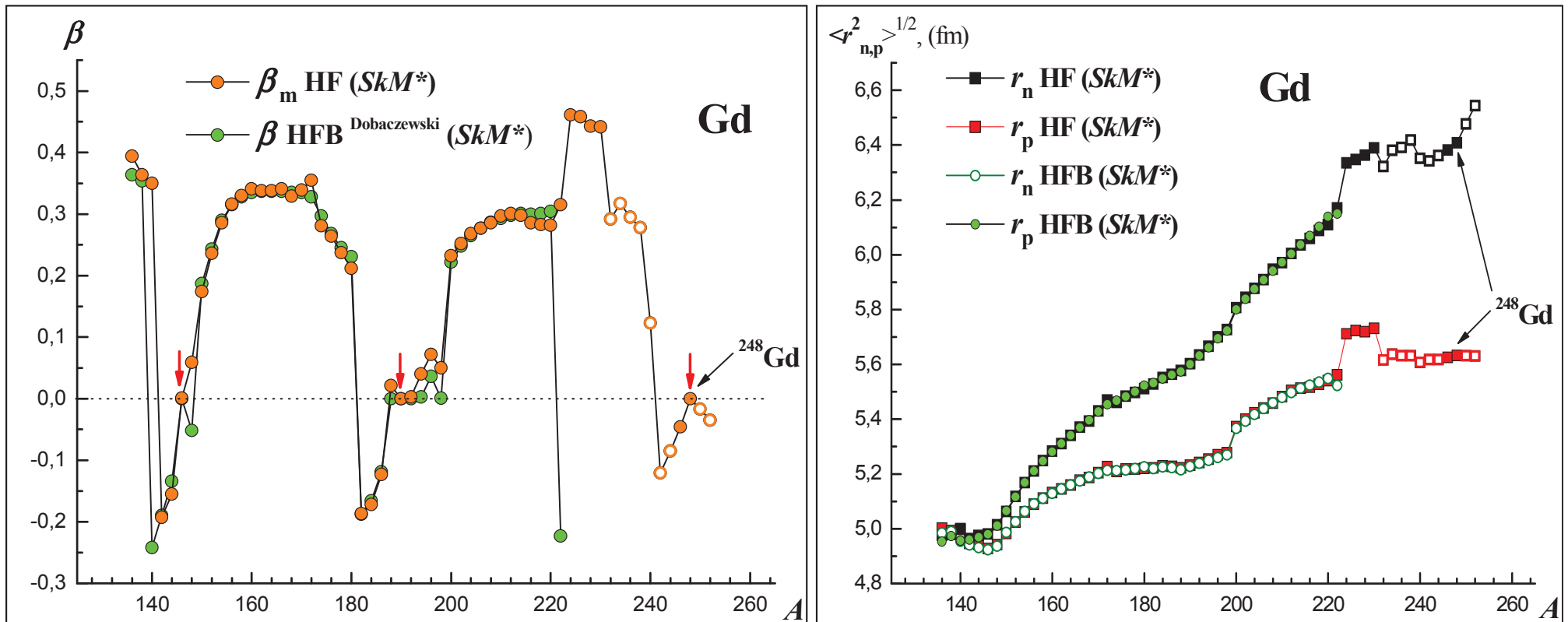


Left: One-neutron separation energies Gd with SkM^* forces compared to HFB calculations [PRC 68 (2003) 054312].
Right: the same for two neutrons separation energy.

Chemical Potential for Gd isotopes

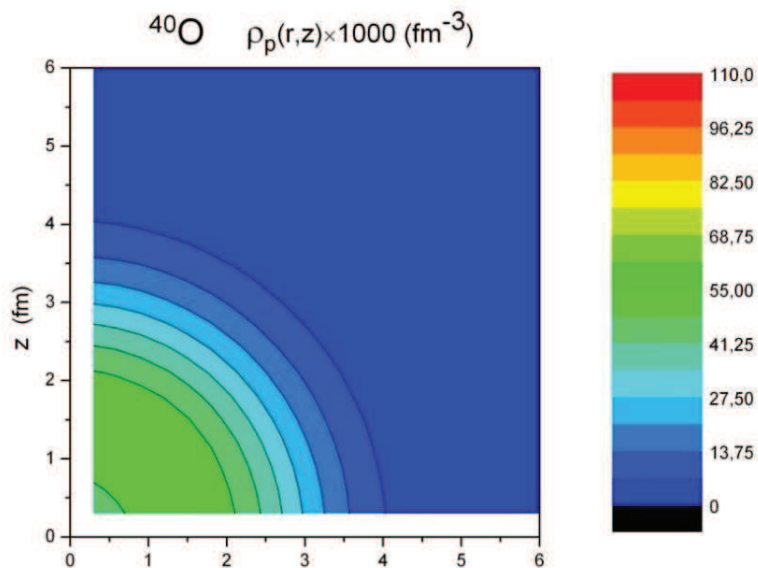
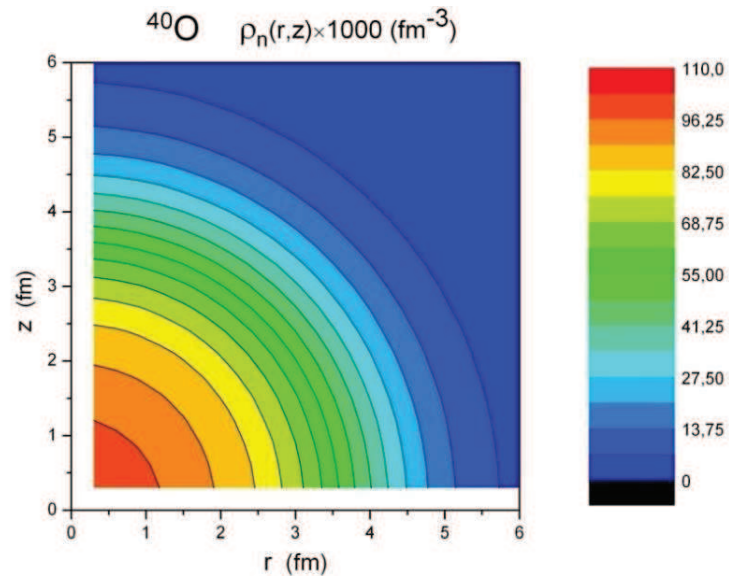


Deformation parameters and Root Mean Square Radii for Gadolinium



- *Empty circles on the left are unstable isotopes.*
- *Isotope ^{248}Gd belongs to the peninsula of stability.*

Proton and neutron density distributions for Oxygen



Interesting relations between proton R_p and neutron R_n root mean square radii (SkM* forces)

For nuclei in the middle of stability valley

$$R_n - R_p \approx 0.1 \div 0.2 \text{ fm}$$

^{40}O

$$R_n - R_p \approx 1.29 \text{ fm}$$

$$R_n / R_p \approx 1.44$$

^{248}Gd

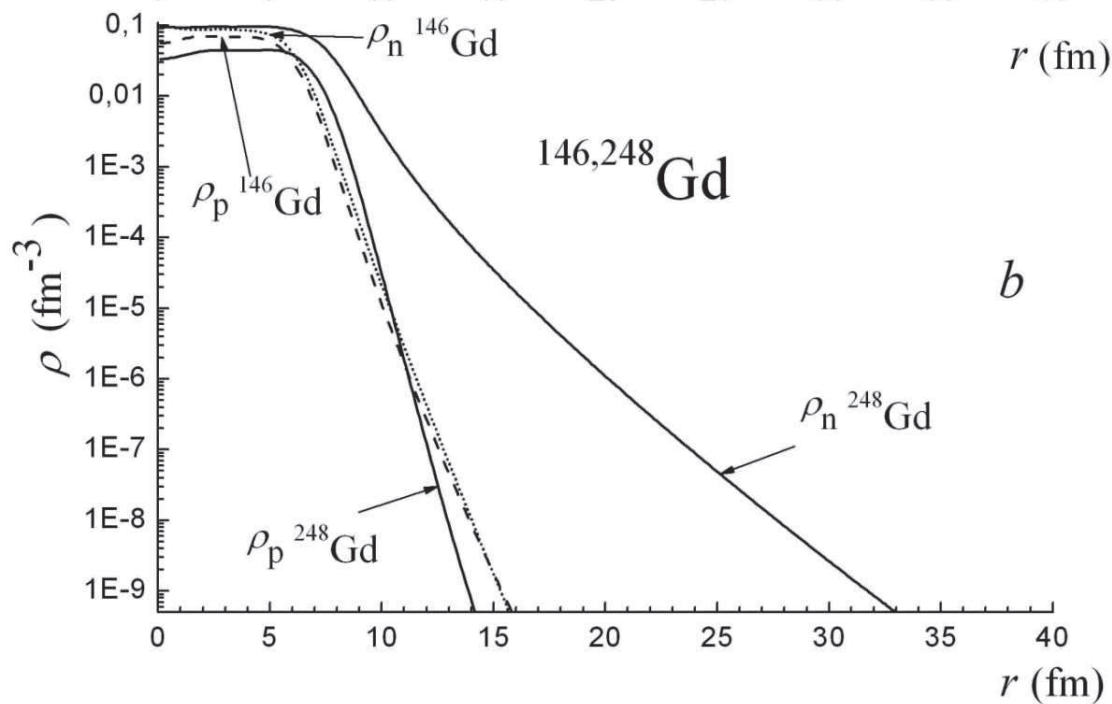
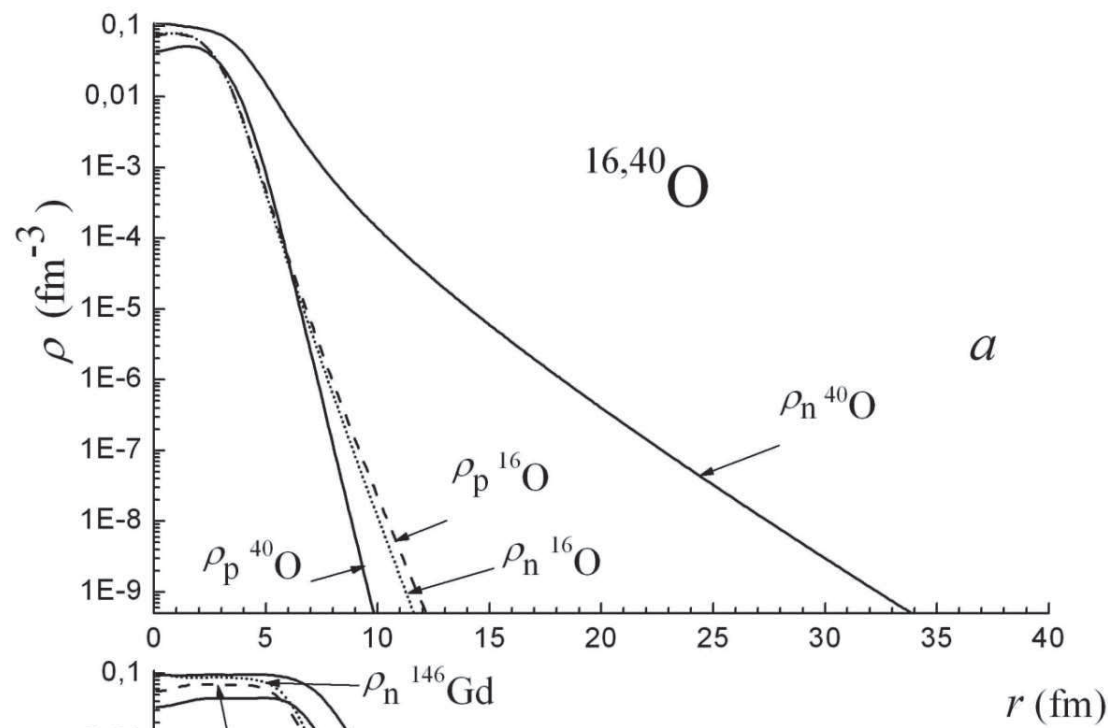
$$R_n - R_p \approx 0.77 \text{ fm}$$

$$R_n / R_p \approx 1.14$$

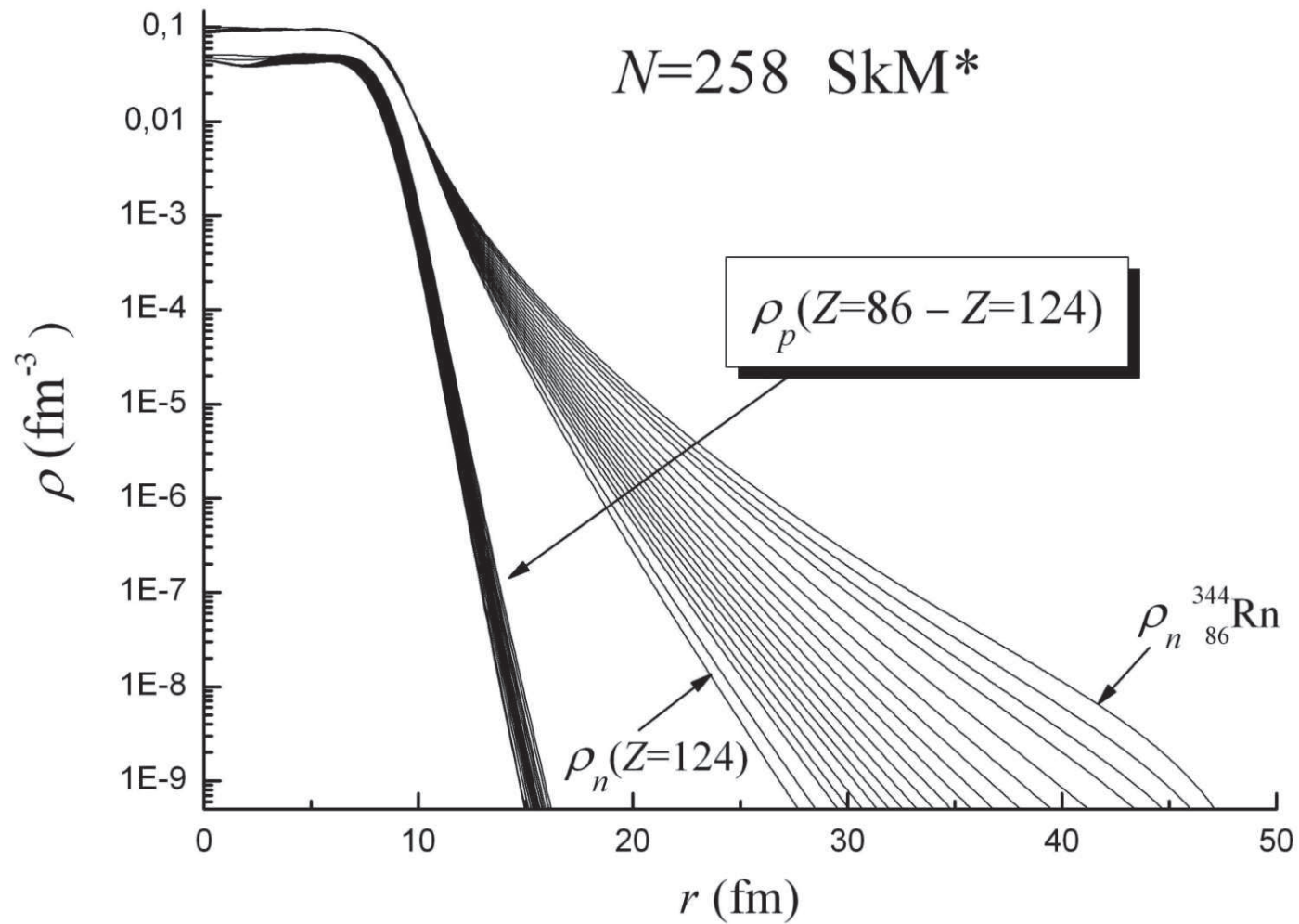
^{240}Ba

$$R_n - R_p \approx 0.94 \text{ fm}$$

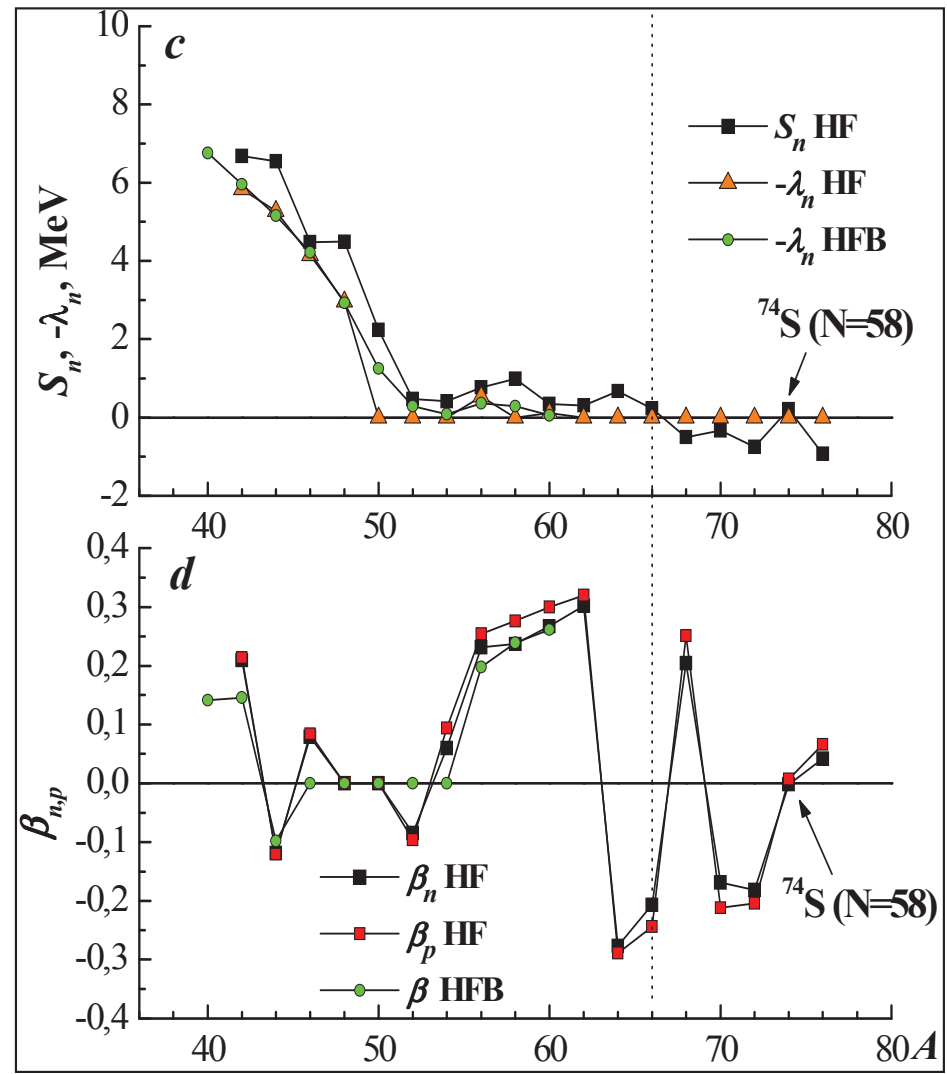
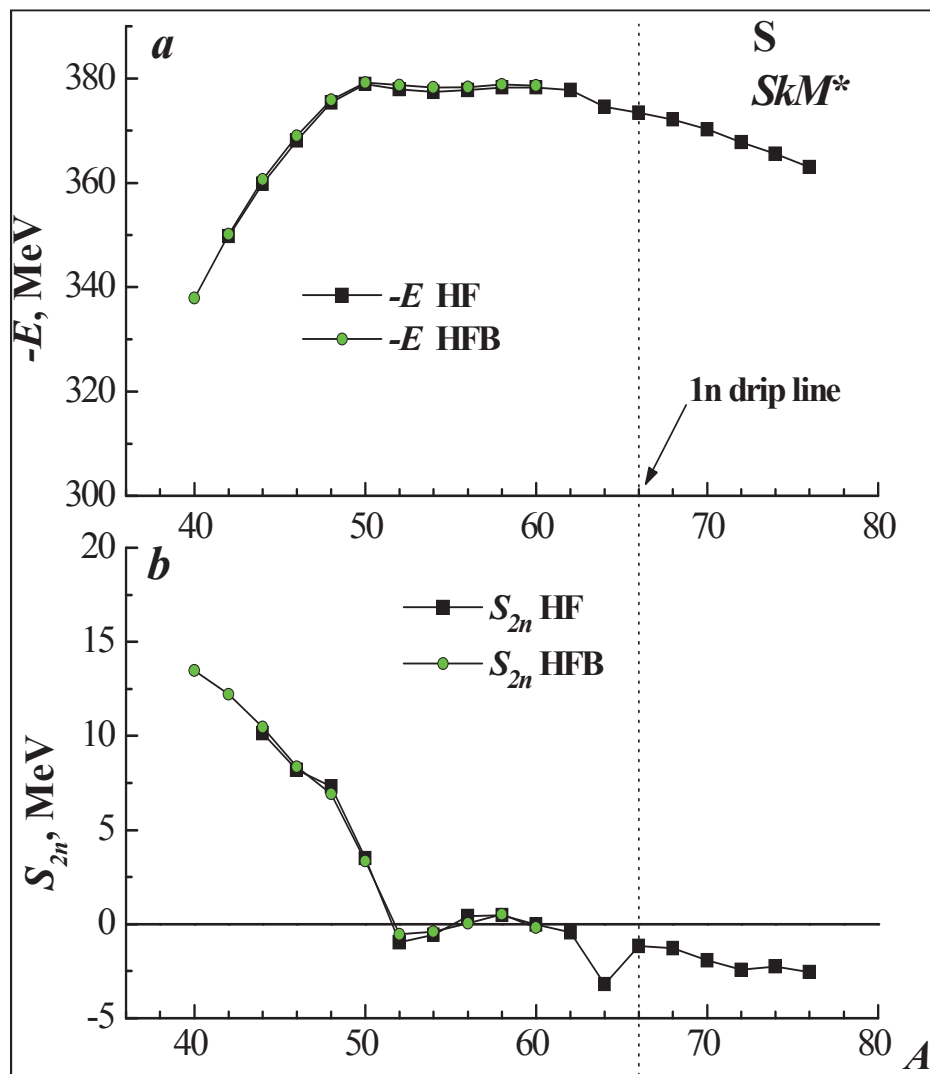
$$R_n / R_p \approx 1.17$$



HF+BCS calculations of proton and neutron density distributions for $^{16,40}\text{O}$ and $^{146,248}\text{Gd}$ with SkM* forces.

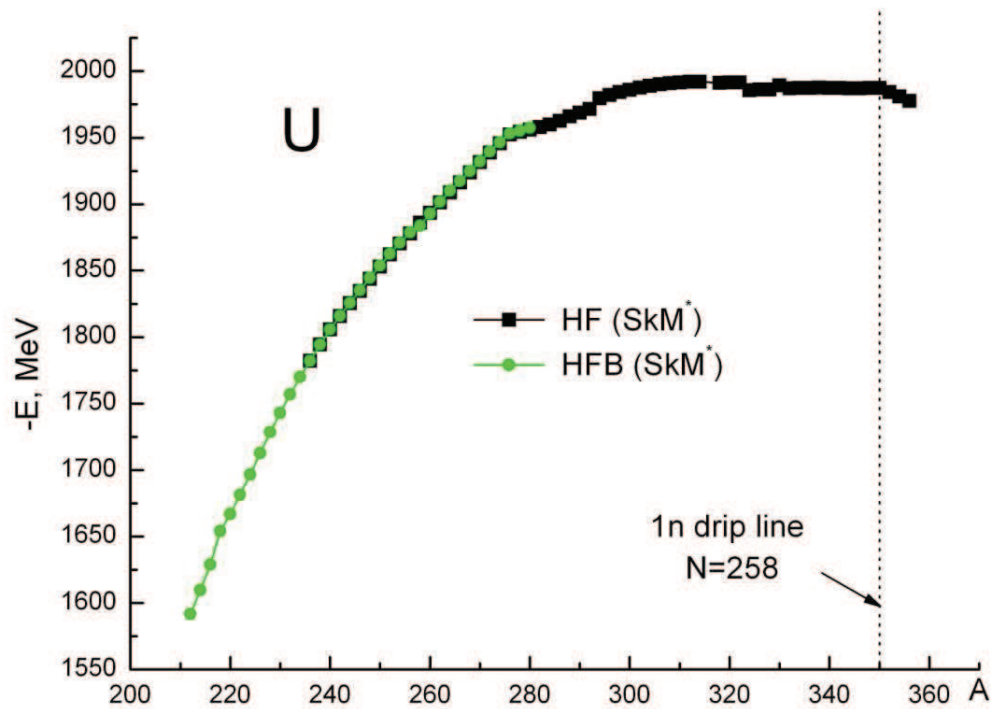


**The same for isotones with N = 258
 from Z=86 (Radon) up to Z=124.**

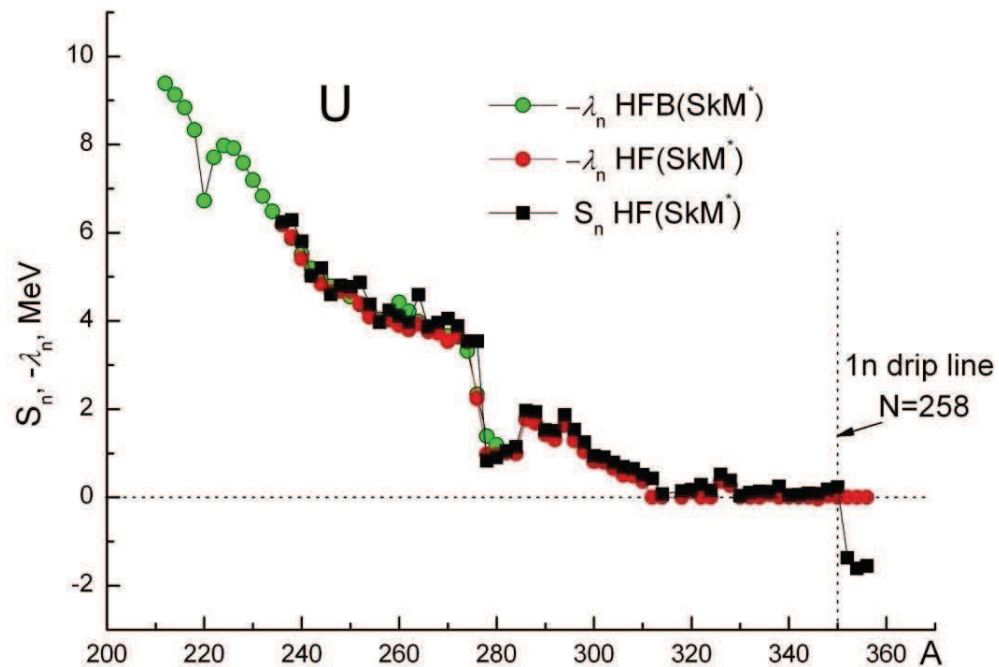


Properties of neutron rich Sulphur calculated by DHF and HFB methods using SkM* forces. Dot line is 1n drip line.

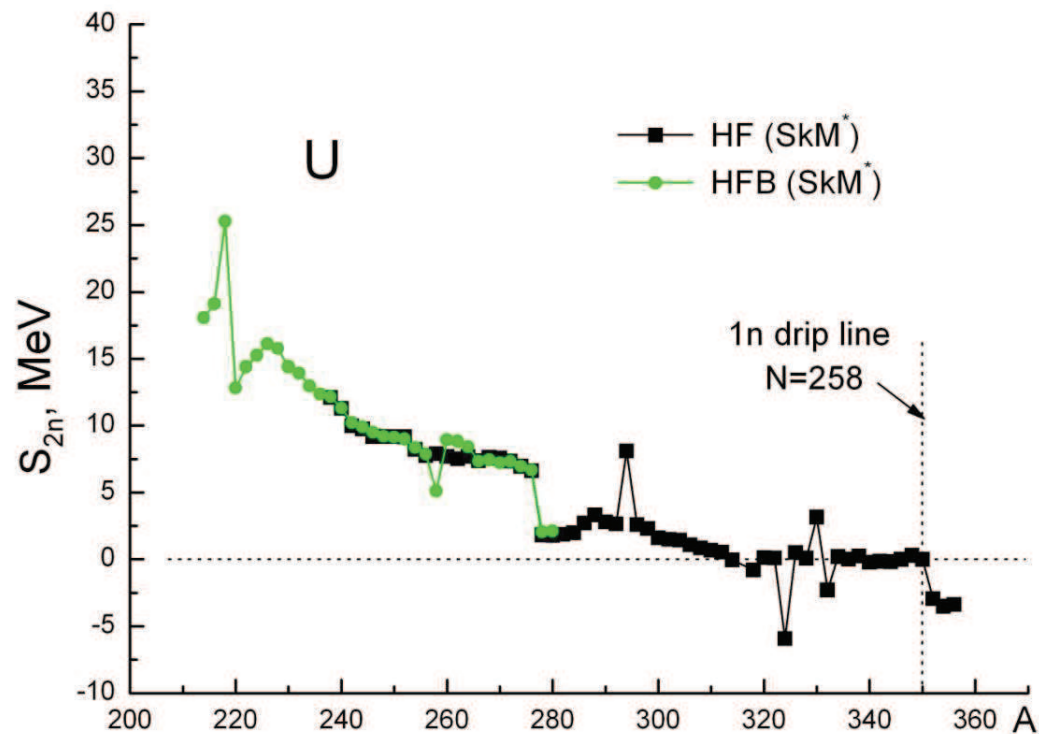
- Fig. (a): Total energy
- Fig.(b): Two-neutron separation energies
- Fig. (c): One-neutron separation energies and chemical potentials
- Fig. (d): Neutron and proton deformation parameters



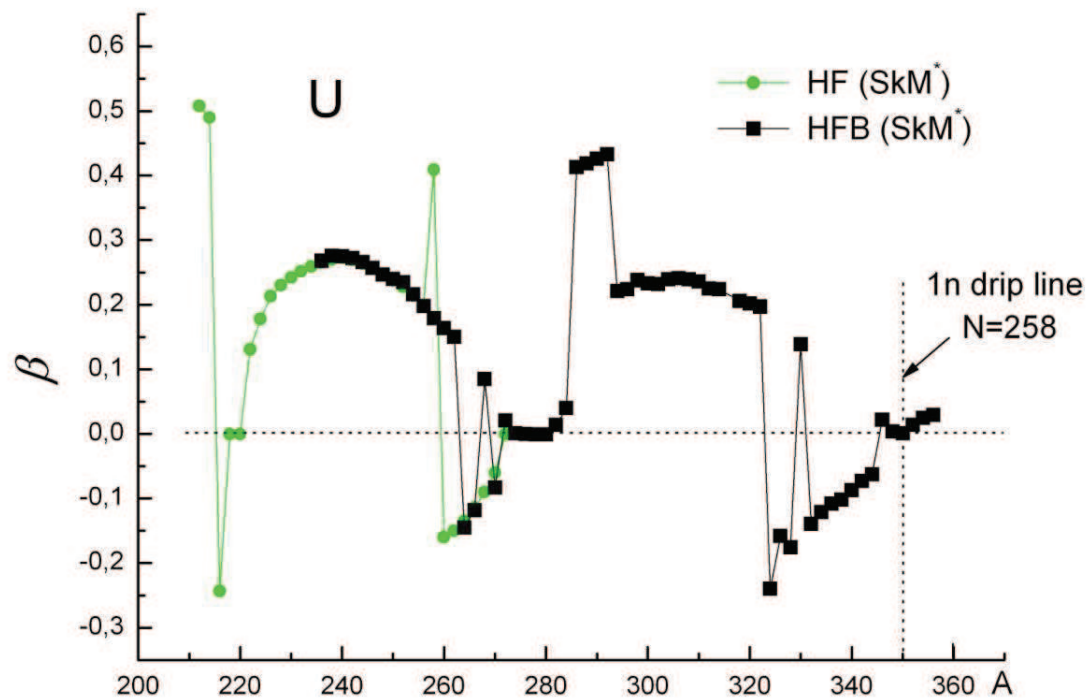
Total energies of uranium isotopes



One-neutron separation energies and neutron chemical potentials of uranium isotopes

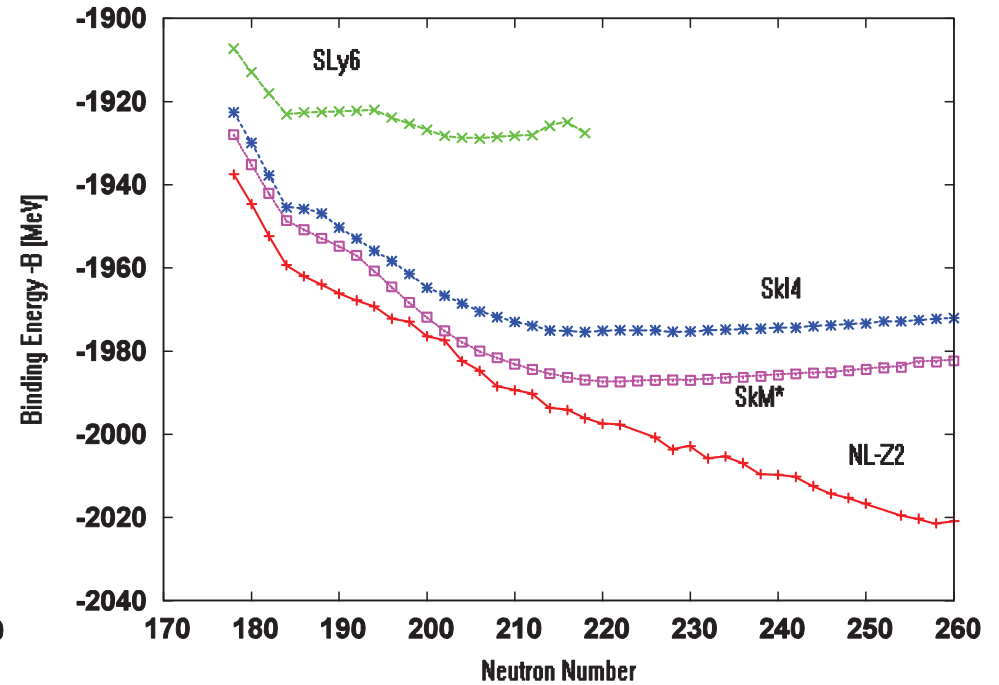
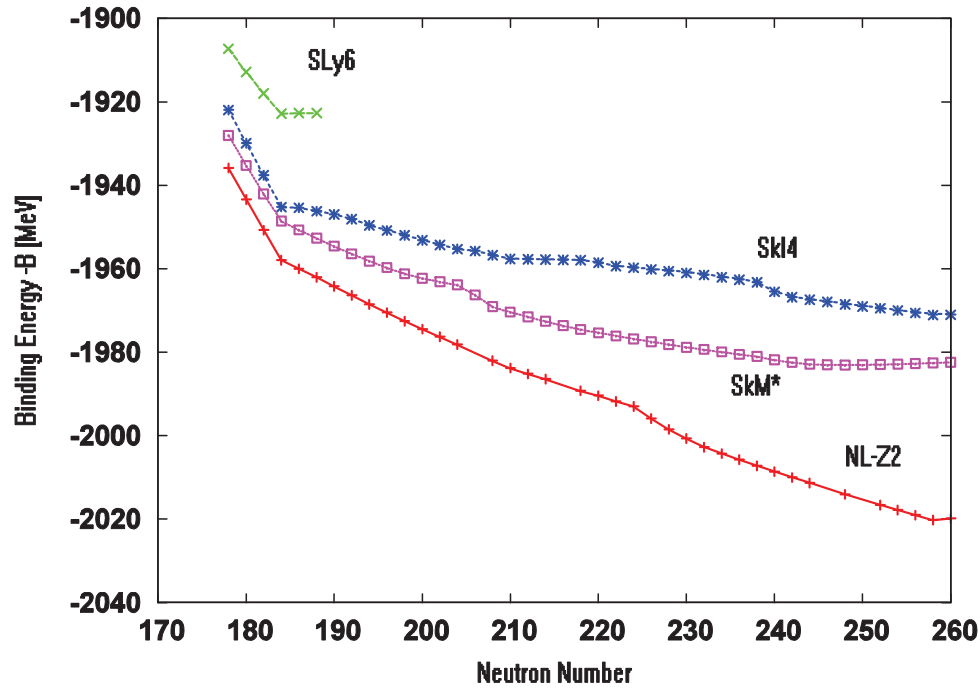


Two-neutron separation energies of uranium isotopes



Parameters of deformation β of uranium isotopes

Which is the heaviest Uranium isotope?



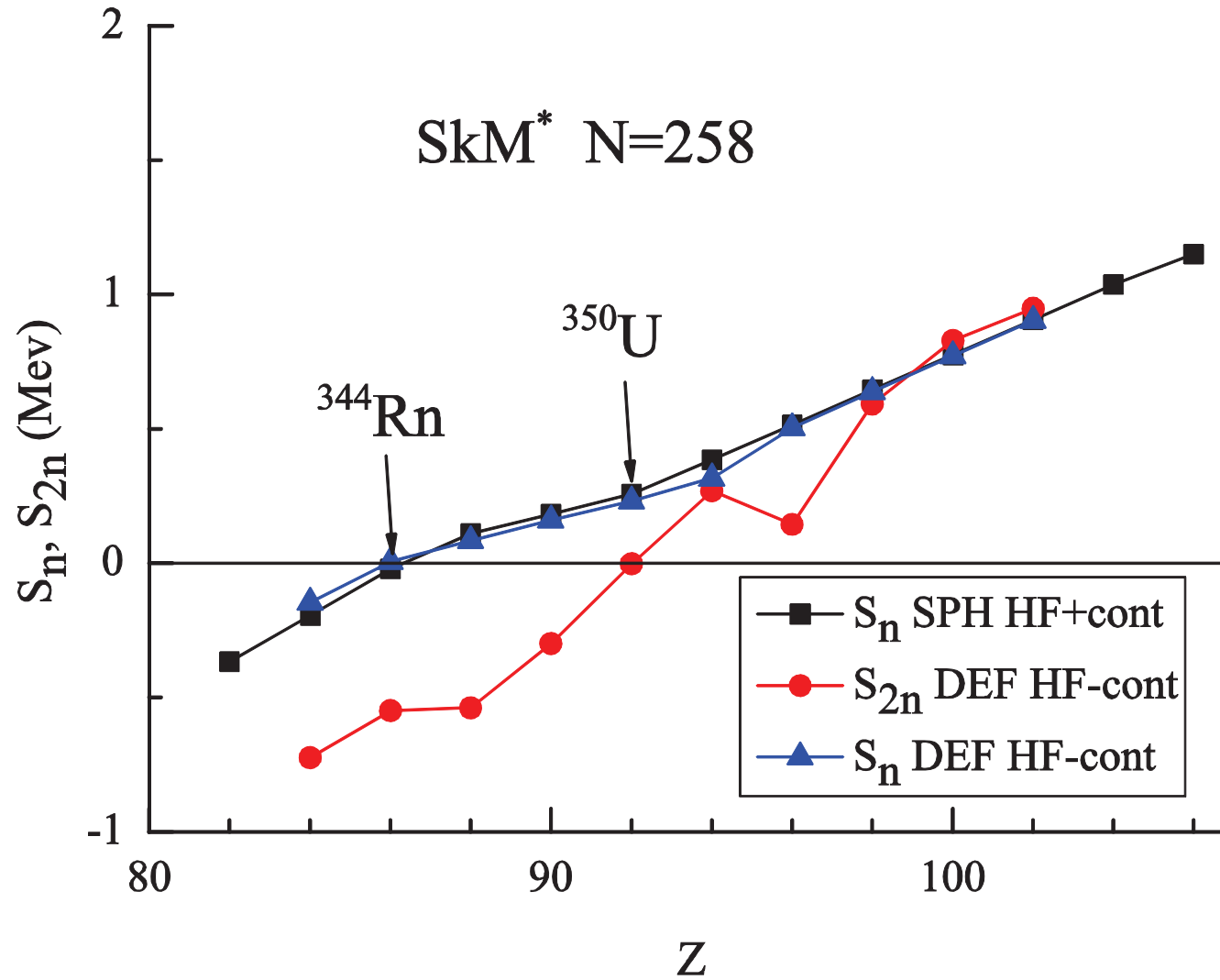
Relativistic mean field and HF+BCS calculation.

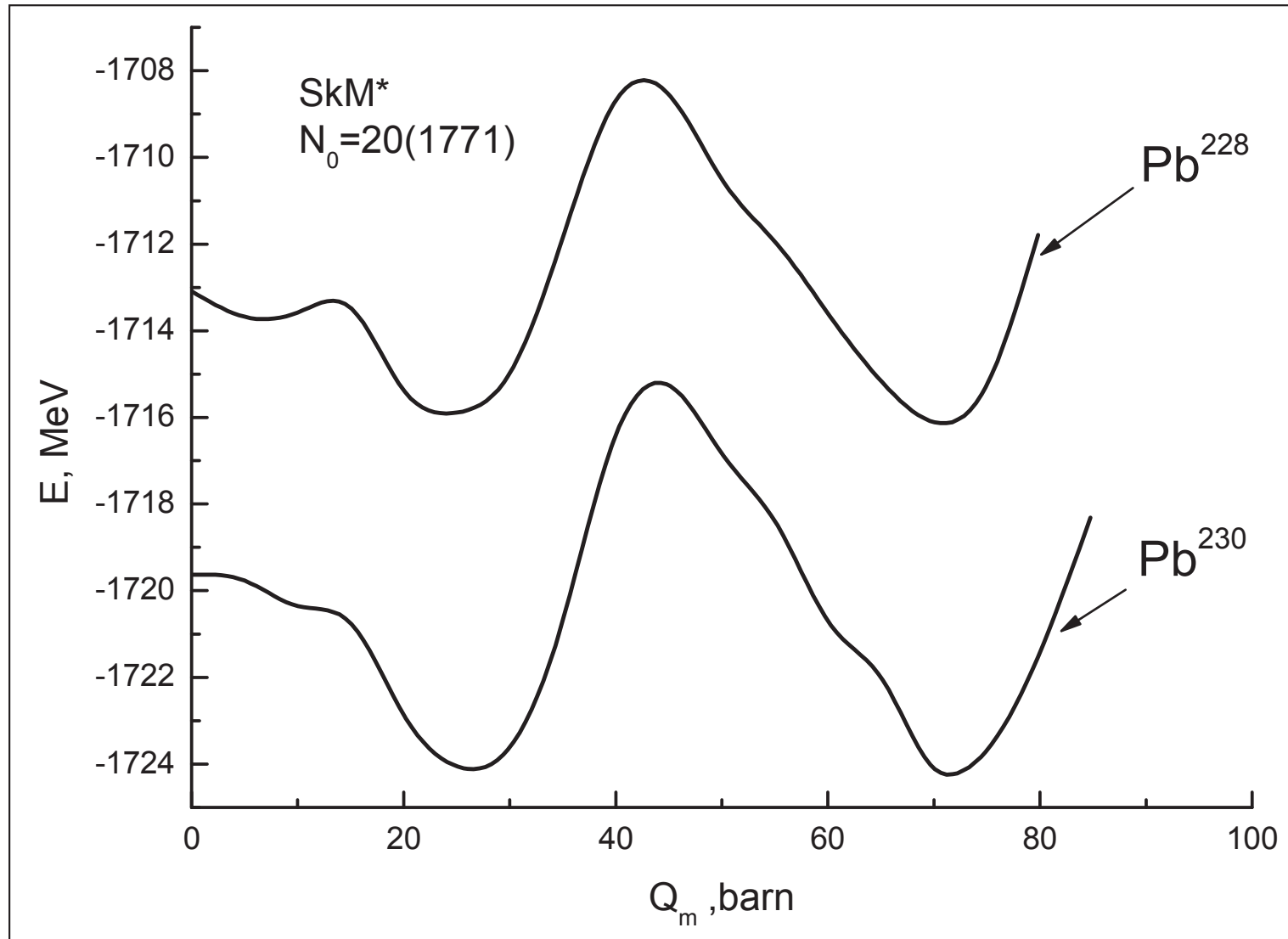
Left: assuming spherical symmetry.

Right: axially deformed case.

Model	N (1d)	N (2d)	Etot (2d)
NL-Z2	258	258	2021 MeV
SkM*	246	220	1987 MeV
SkI4	258	218	1975 MeV
SLy6	184	206	1929 MeV

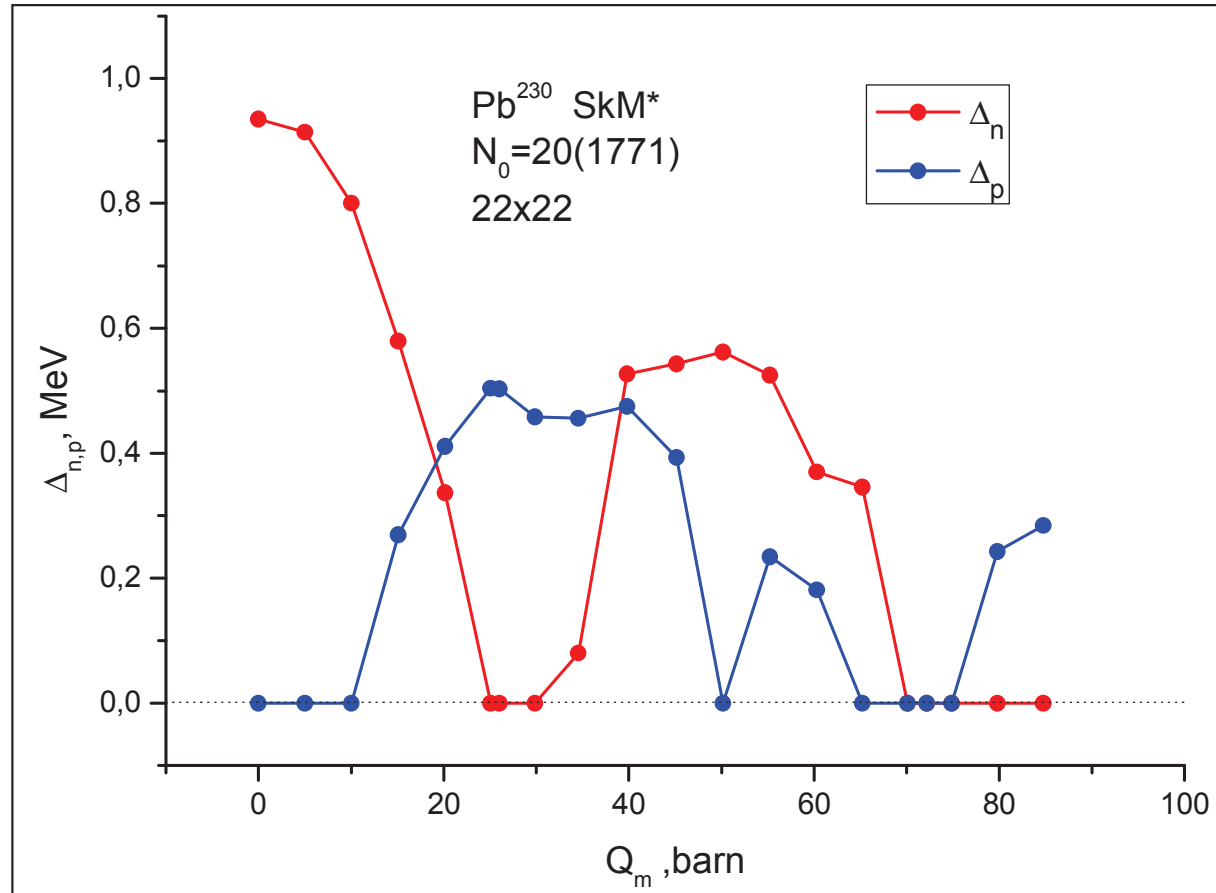
Peninsula on the shell N=258

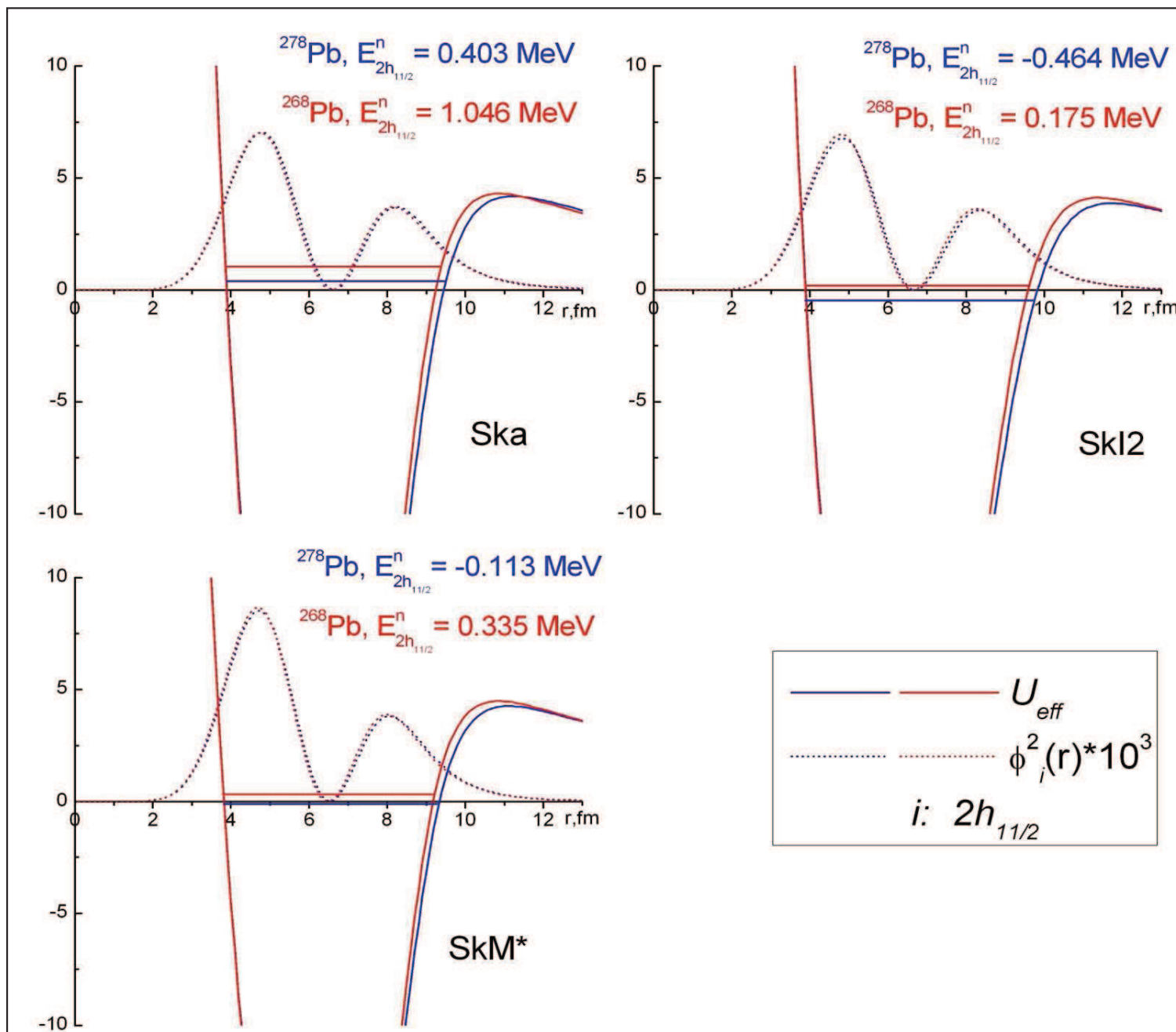




Constrained HF calculations of $^{228,230}\text{Pb}$ energy surface using Ska forces.

Energy gaps of ^{230}Pb using SkM forces.*



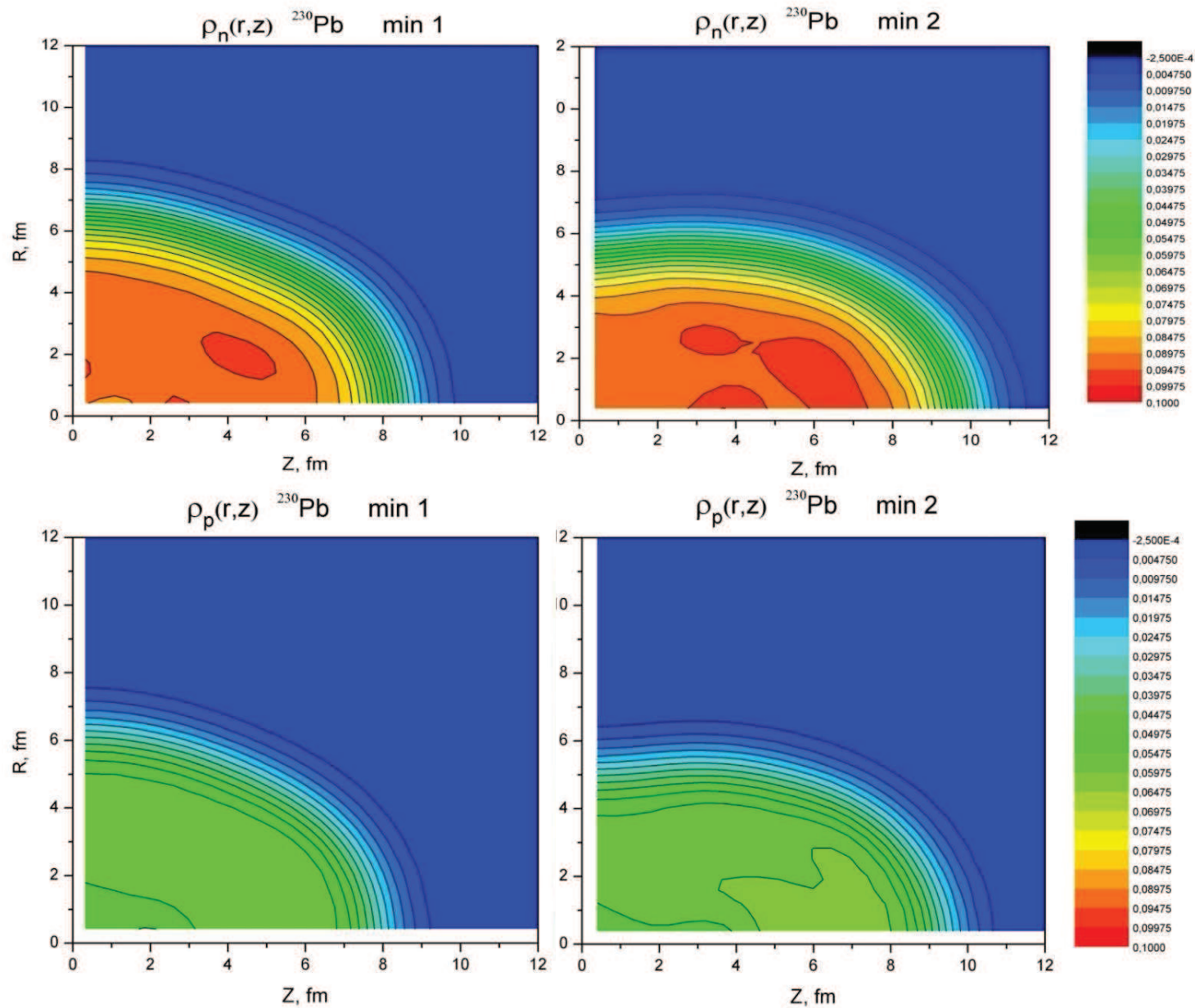


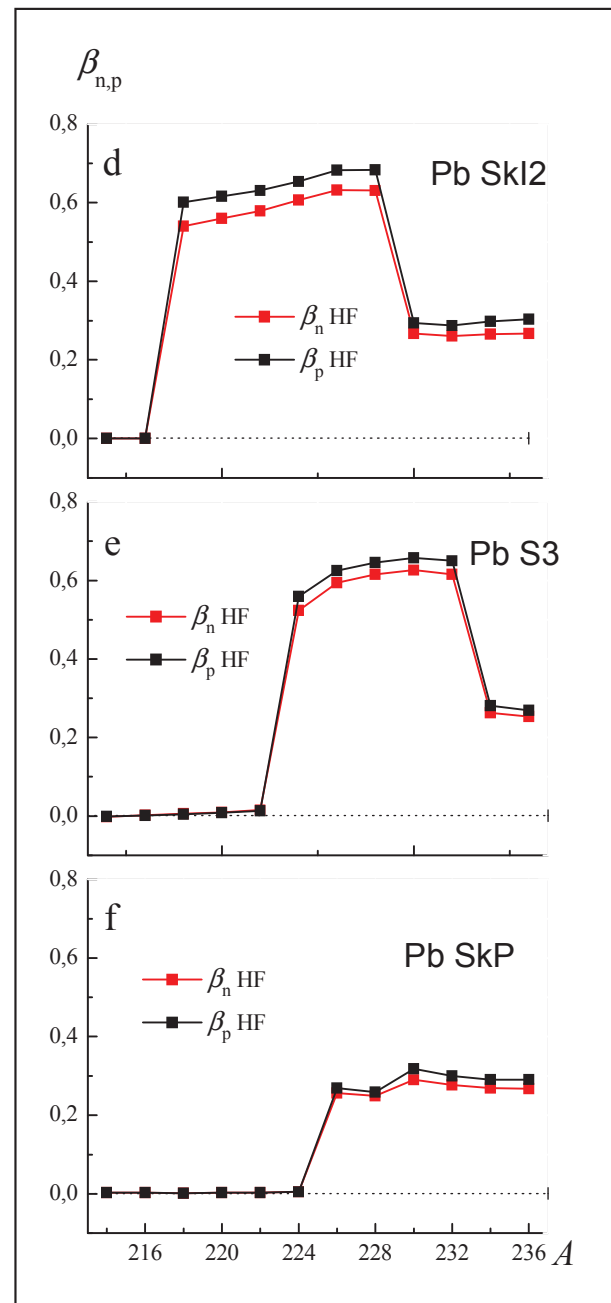
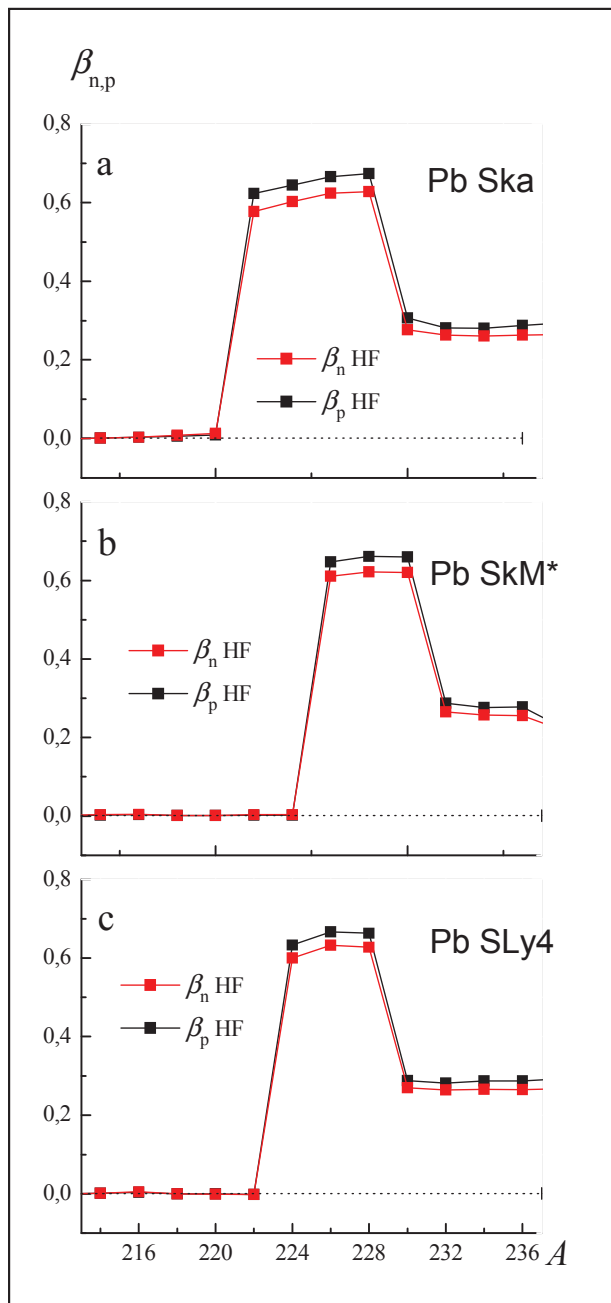
Mechanism of stability enhancement on the example of Pb isotopes

Density distribution in ^{230}Pb

Left: normally deformed

Right: superdeformed





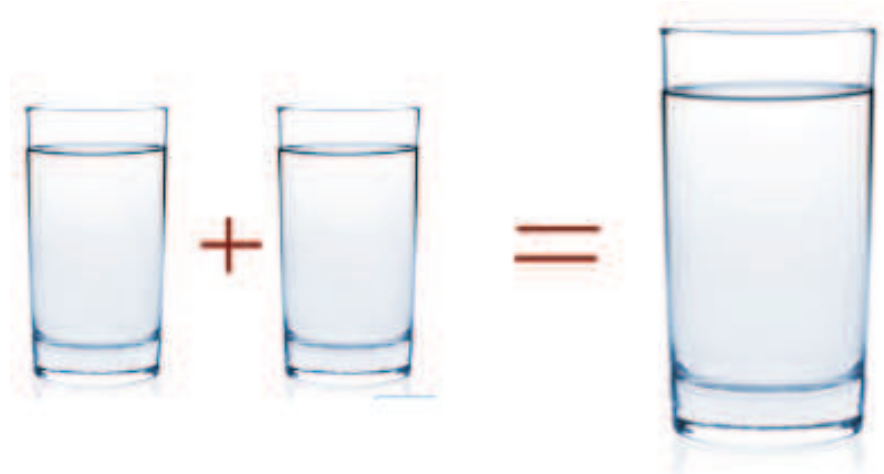
Proton and neutron deformation parameters using Ska, SkM*, SkI2, S3 and SkP forces

Conclusions

- The *peninsulas* of nuclei stable with respect to emission of one or two neutrons can exist beyond the drip line that was previously known theoretically.
- The numbers N which correspond to the *peninsulas* of stability are close or coincide with the known magic numbers.
- The stability restoration through adding more neutrons and formation of stability *peninsulas* appear for various Skyrme forces.
- The isotones with $N=32, 58, 82, 126, 184$ which belong to the *peninsulas* of stability have spherical shape.
- The mechanism of stability restoration is due to the complete filling of neutron subshells lying in the discrete spectrum and having large values of angular momentum. These shells being partially filled are located in the continuum.
- Our results are in a good agreement with the results obtained by the HFB method with Skyrme forces up to neutron drip line .
- The obtained results show that the structure of the drip-line can be rather complex and reflects the shell structure. The drip line may extend further beyond what it was generally assumed previously.

Stability of matter around us

Thermodynamics: the energy is an extensive quantity



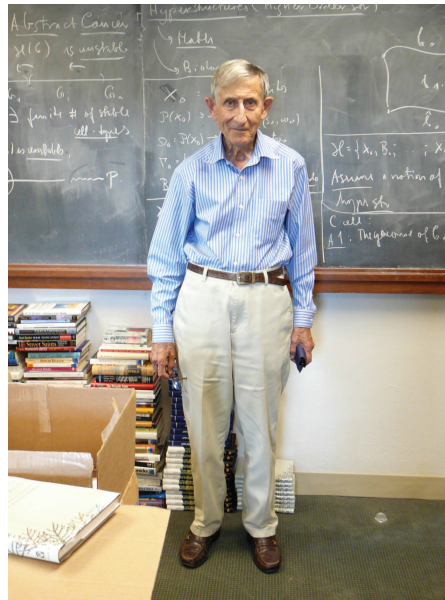
$$\lim_{N \rightarrow \infty} E(N)/N = e_0 \quad \text{Exists,}$$

where N is the number of atoms. With pointwise nuclei and electrons $E(N)$ is a mathematically well defined quantity. Stability implies that there exist $c, C > 0$ such that

$$cN \leq E(N) \leq CN$$

Proof of Dyson and Lenard

In 1967 John Freeman Dyson and Andrew Lenard presented a mathematical proof of matter's stability.



Without the Pauli principle the matter is not stable, since without it $E(N) \simeq N^{5/3}$. That is, the assembly of any two macroscopic objects would release energy comparable to that of an atomic bomb.

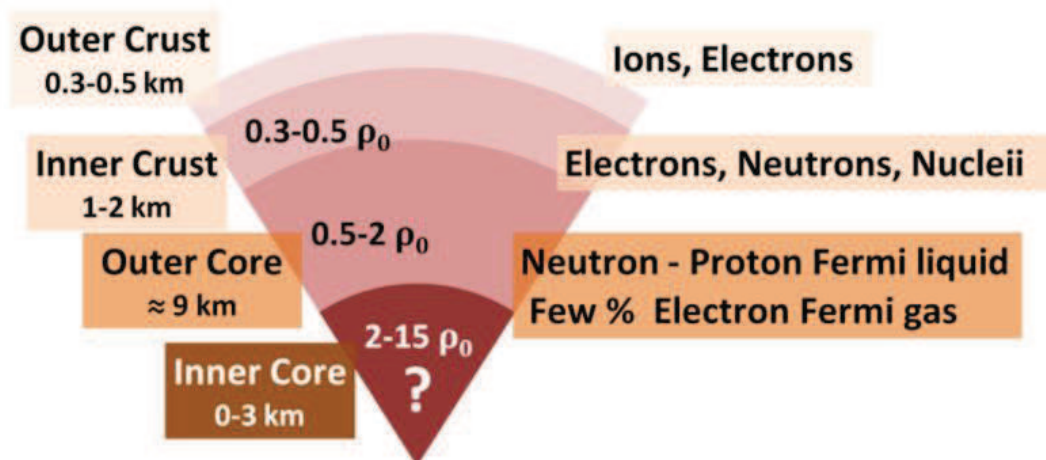
Protons and Neutrons also Form Matter

- ▶ For finite nuclei with N neutrons and Z protons ($A = Z + N$) one has Bethe-Weizsäcker formula

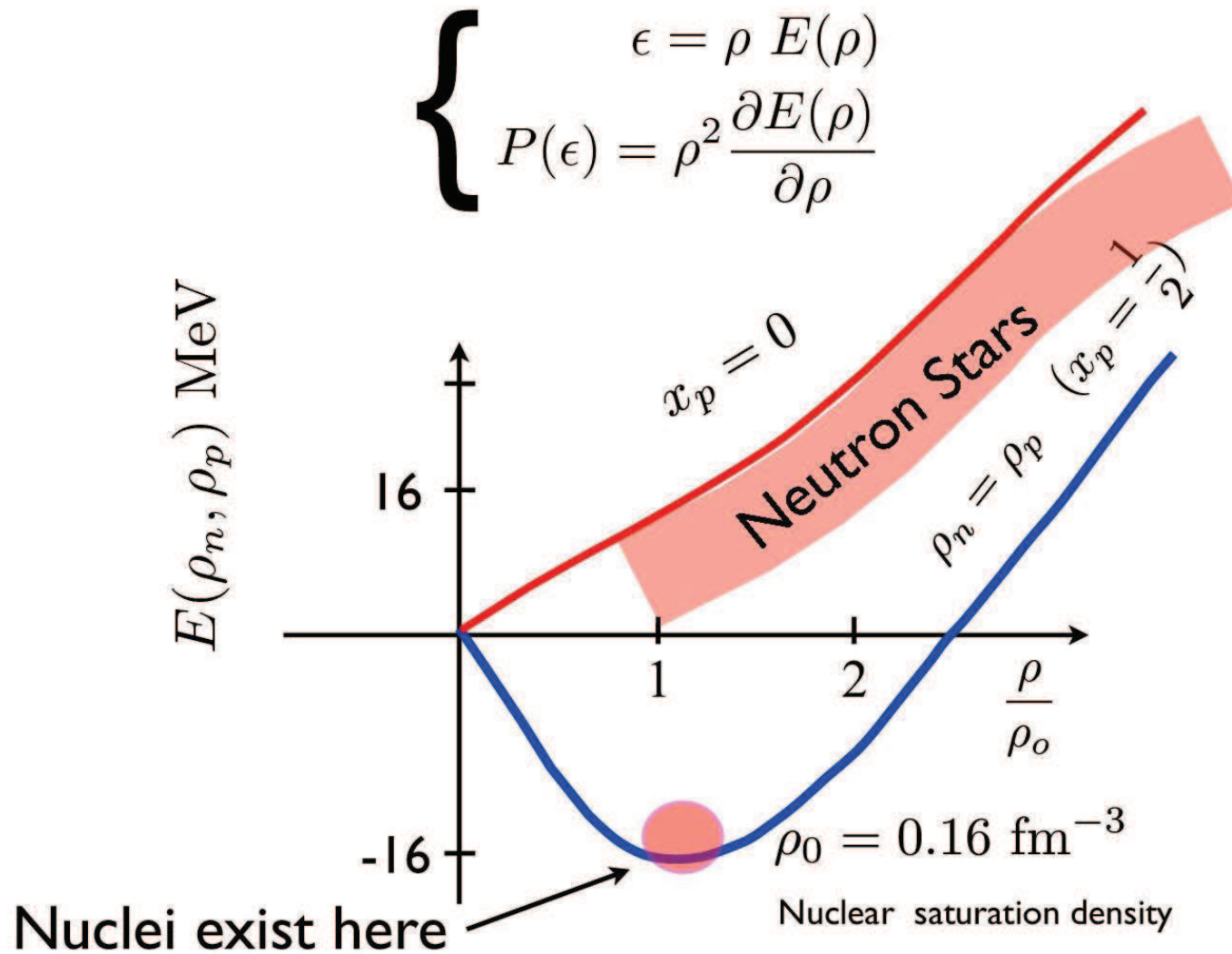
$$E = a_V A - a_S A^{2/3} - a_A \frac{(A - 2Z)^2}{A} - \delta(A, Z), \quad (7)$$

where we assume zero Coulomb forces.

- ▶ For large N with gravitational forces we observe neutron stars



Masses and Radii of the Stars are governed by Equation of State



Nuclear Hamiltonian

$$H = \sum_i K_i + \sum_{i<j} v_{ij} + \sum_{i<j<k} V_{ijk}$$

K_i : Non-relativistic kinetic energy, $m_n - m_p$ effects included

v_{ij} : Argonne v18 (1995)

$$v_{ij} = v_{ij}^\gamma + v_{ij}^\pi + v_{ij}^R + v_{ij}^{CIB}$$

v_{ij}^γ : pp , pn & nn electromagnetic terms, Coulomb, magnetic, etc. with form factors

$v_{ij}^\pi \sim [Y(r_{ij})\sigma_i \cdot \sigma_j + T(r_{ij})S_{ij}] \otimes \tau_i \cdot \tau_j$; $\langle v_{ij}^\pi \rangle$ contributes $\sim 85\%$ of $\langle v_{ij} \rangle$

$$v_{ij}^R = \sum_{p=1,14} v_p(r_{ij}) O_{ij}^p$$

$$O_{ij}^{p=1,14} = [1, \sigma_i \cdot \sigma_j, S_{ij}, \mathbf{L} \cdot \mathbf{S}, \mathbf{L}^2, \mathbf{L}^2 \sigma_i \cdot \sigma_j, (\mathbf{L} \cdot \mathbf{S})^2] \otimes [1, \tau_i \cdot \tau_j]$$

Determined phenomenologically

v_{ij}^{CIB} : 4 operators for nuclear charge independence breaking

AV18 is a direct fit to the Nijmegen data base:

1787 pp , 2514 pn , 1 nn data for $E_{Lab} < 350$ MeV ~ 40 parameters; $\chi^2/\text{d.o.f.} = 1.09$

Typical of modern NN potentials

Three-Body Force

Nucleons are not elementary particles!

Three-body force is **NOT** an iteration of the two-body force

Two-body force



Three-Body Force

Nucleons are not elementary particles!

Three-body force is **NOT** an iteration of the two-body force

Two-body force



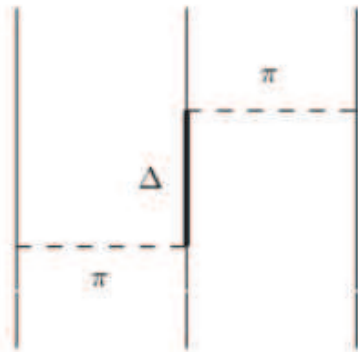
Three-body force



Urbana IX Three-Body Potential

UIX contains **two contributions**

$V^{2\pi}$ – Fujita Myiazawa



Cyclic sum of three permutations

$$V^{2\pi} = A^{2\pi} (O_{123}^{2\pi} + O_{231}^{2\pi} + O_{312}^{2\pi})$$

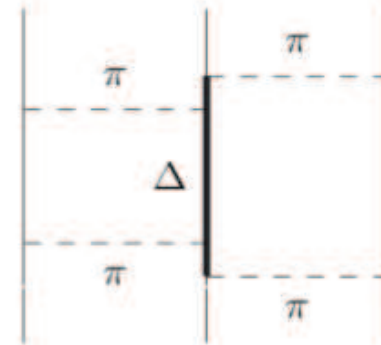
$$O_{123}^{2\pi} = \left(\{\hat{X}_{12}, \hat{X}_{23}\} \{\tau_{12}, \tau_{13}\} + \frac{1}{4} [\hat{X}_{12}, \hat{X}_{23}] [\tau_{12}, \tau_{23}] \right)$$

$$\hat{X}_{ij} = Y(m_\pi r) \sigma_{ij} + T(m_\pi r) S_{ij}$$



Cutoff functions of OPE

V^R – scalar repulsive term



Cyclic sum of three permutations

$$V^R = U_0 \sum_{cycl} T^2(m_\pi r_{12}) T^2(m_\pi r_{23})$$



Cutoff Functions of OPE

The functions $T(r)$, $Y(r)$ are given through

$$Y(r) = \frac{e^{-\mu r}}{\mu r} [1 - e^{-br^2}],$$

$$T(r) = \left(1 + \frac{3}{\mu r} + \frac{3}{\mu^2 r^2}\right) \frac{e^{-\mu r}}{\mu r} [1 - e^{-br^2}]^2.$$

Here $\mu = (m_{\pi_0} + 2m_{\pi_{\pm}})c/(3\hbar)$ is the average of the pion masses and $b = 2.0 \text{ fm}^{-2}$.

Expanding the exponents it is easy to see that $T(0) = Y(0) = 0$, which means that **the whole three-body interaction vanishes if three nucleons occupy the same position in space!** Urbana VI does not have that problem.

Form-Factors in Electrostatics

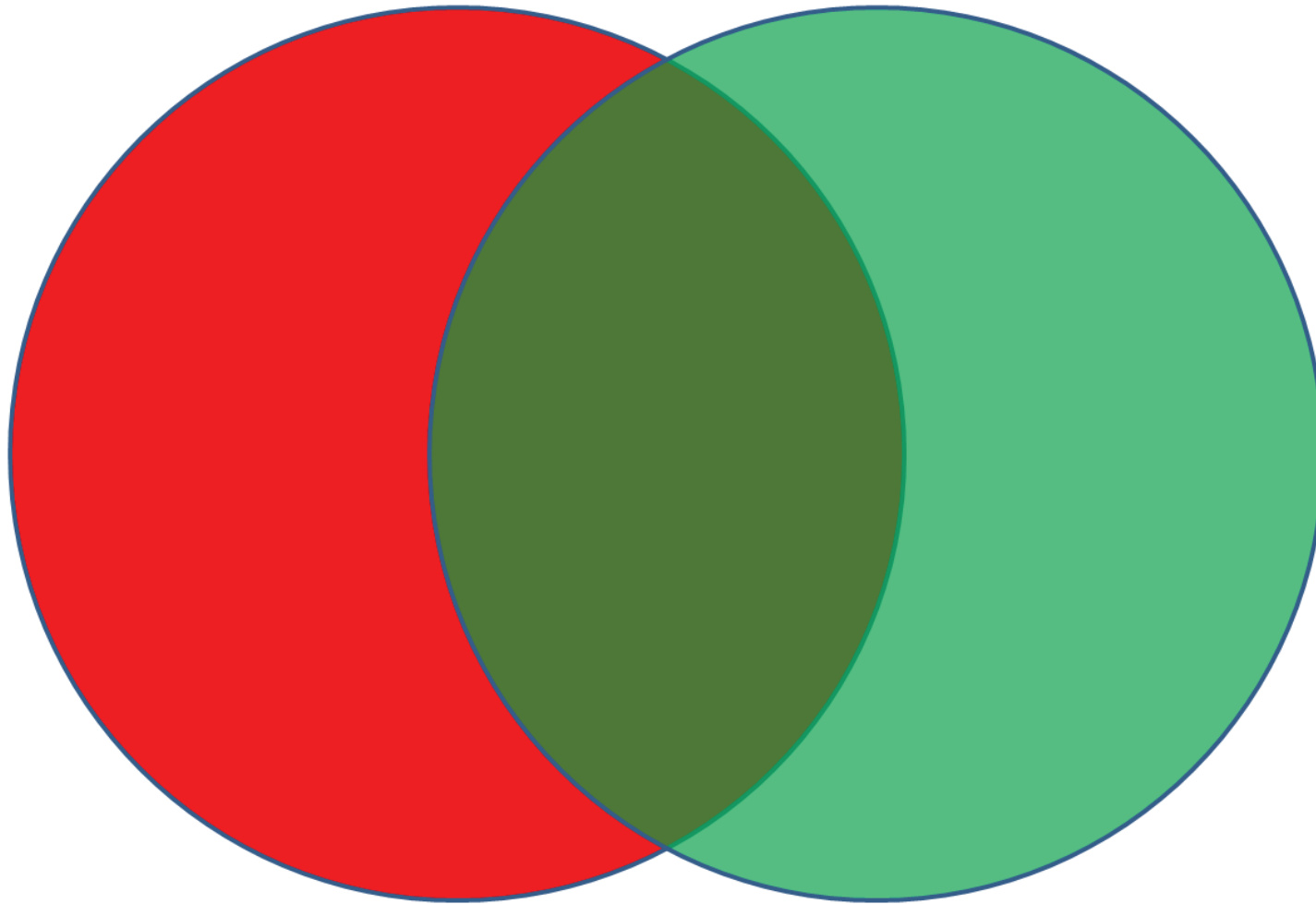


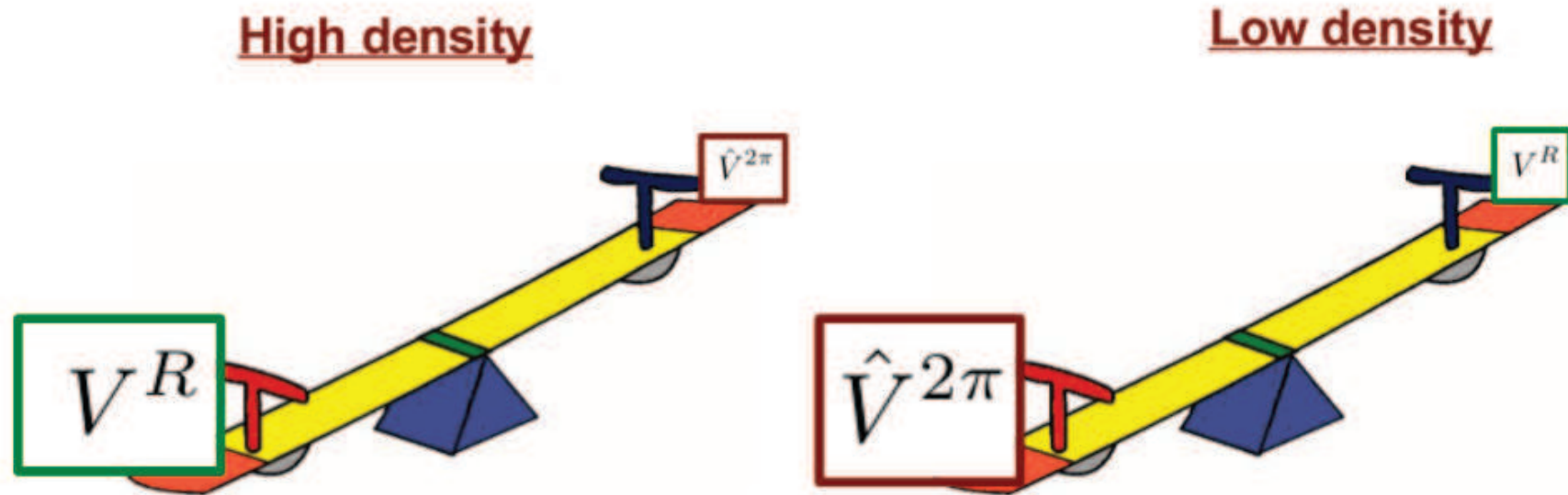
Figure: Identically uniformly charged spheres repel each other but the repulsion is zero when the spheres overlap completely.

Urbana IX Three-Body Potential

UIX potential has two parameters

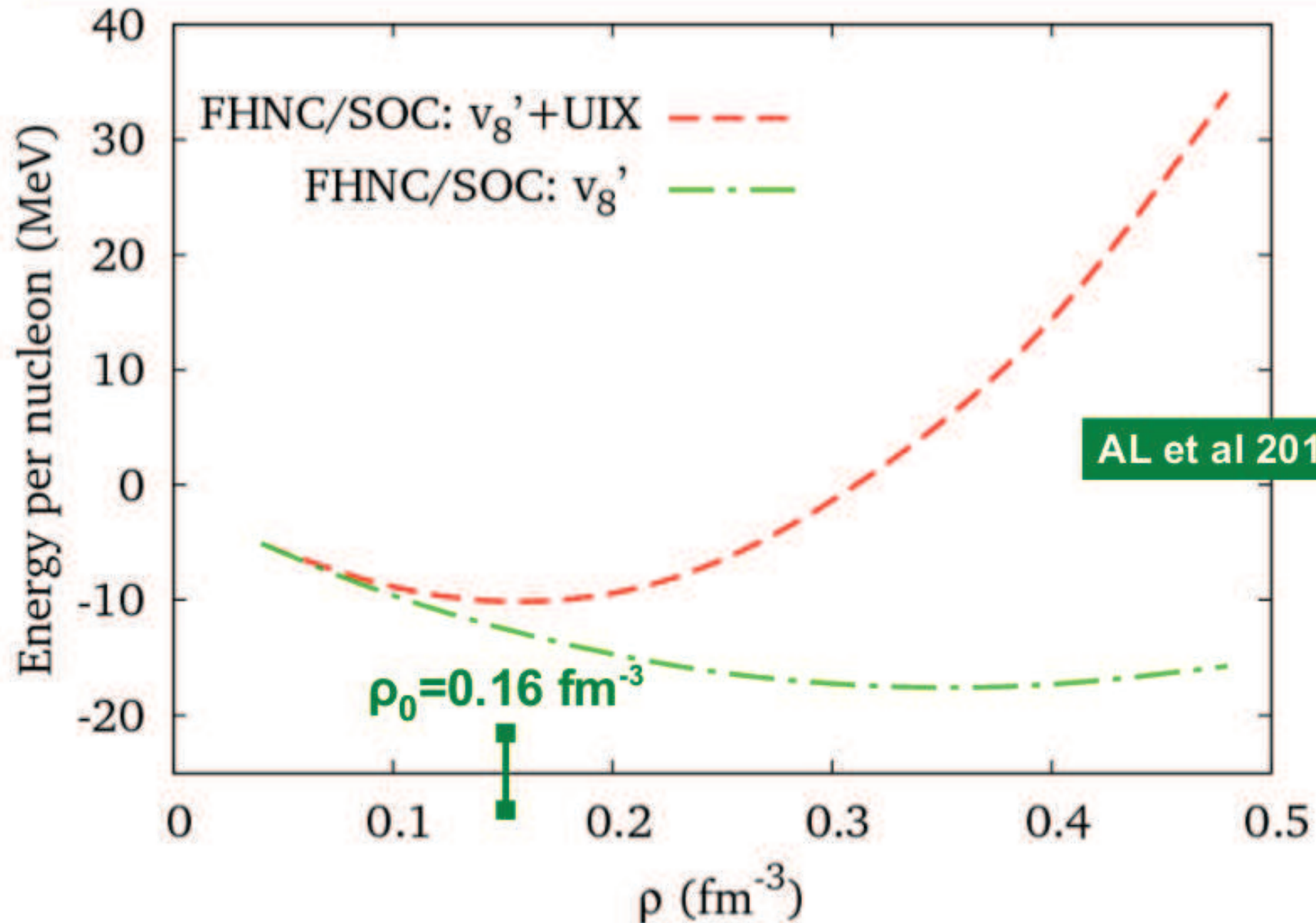
- $A^{2\pi}$ adjusted to reproduce the observed binding energies of ${}^3\text{H}$.
- U_0 tuned for FHNC/SOC calculations to reproduce the empirical equilibrium density of SNM

Lagaris and Pandharipande argued that, because of correlations, the relative weight of the contribution depends upon the density of the system:



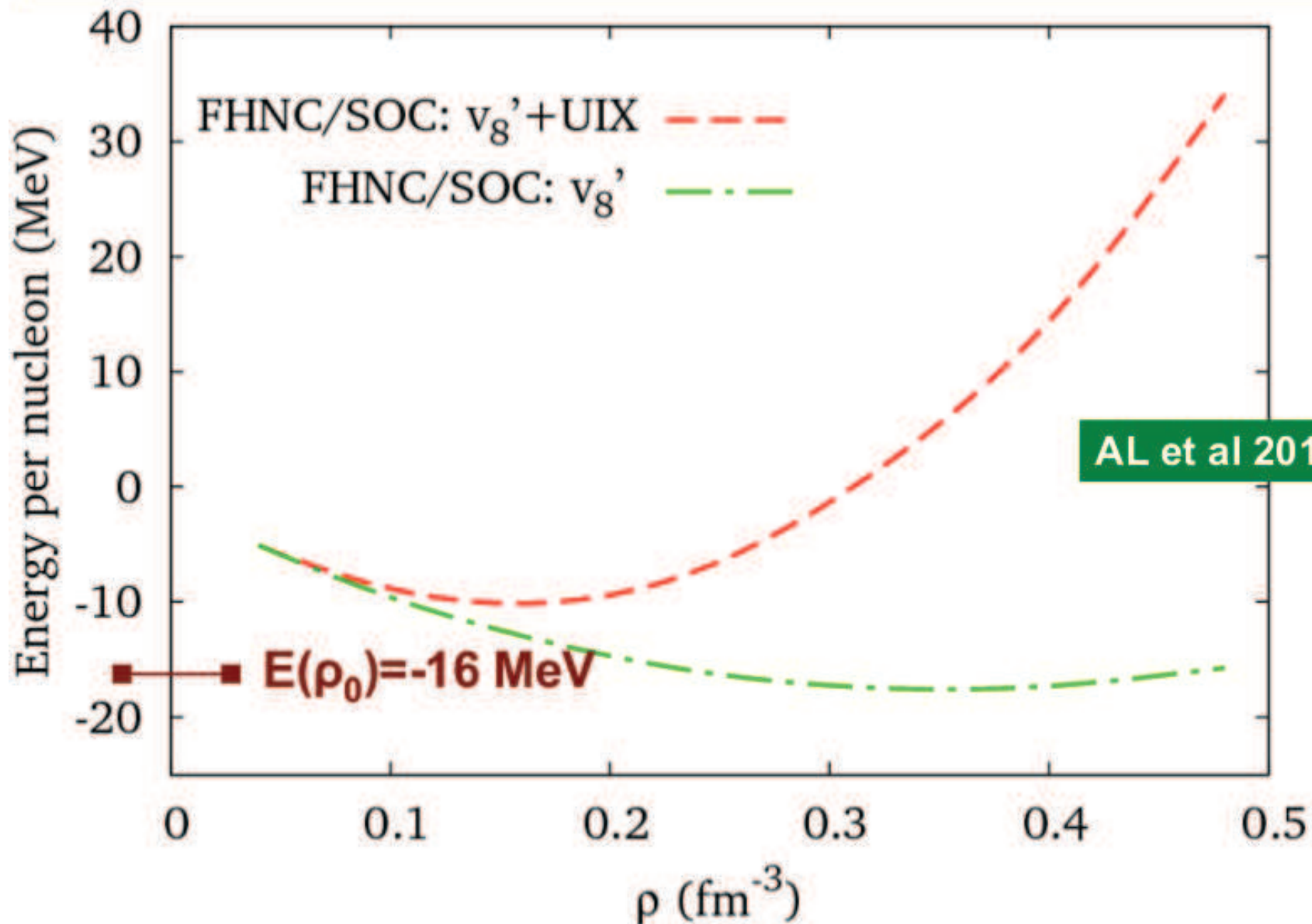
Urbana IX Three-Body Potential

SNM saturation density is well reproduced

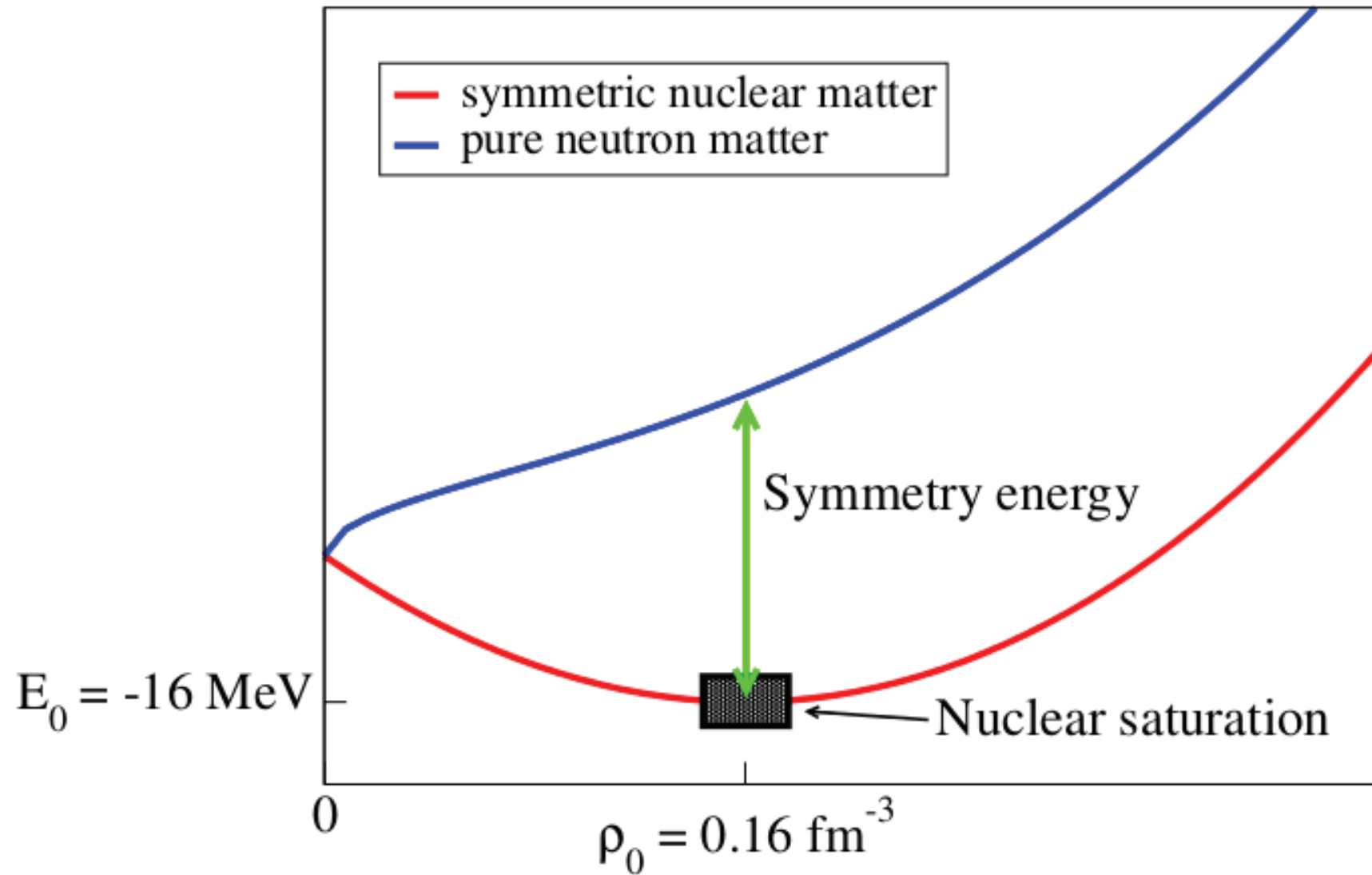


Urbana IX Three-Body Potential

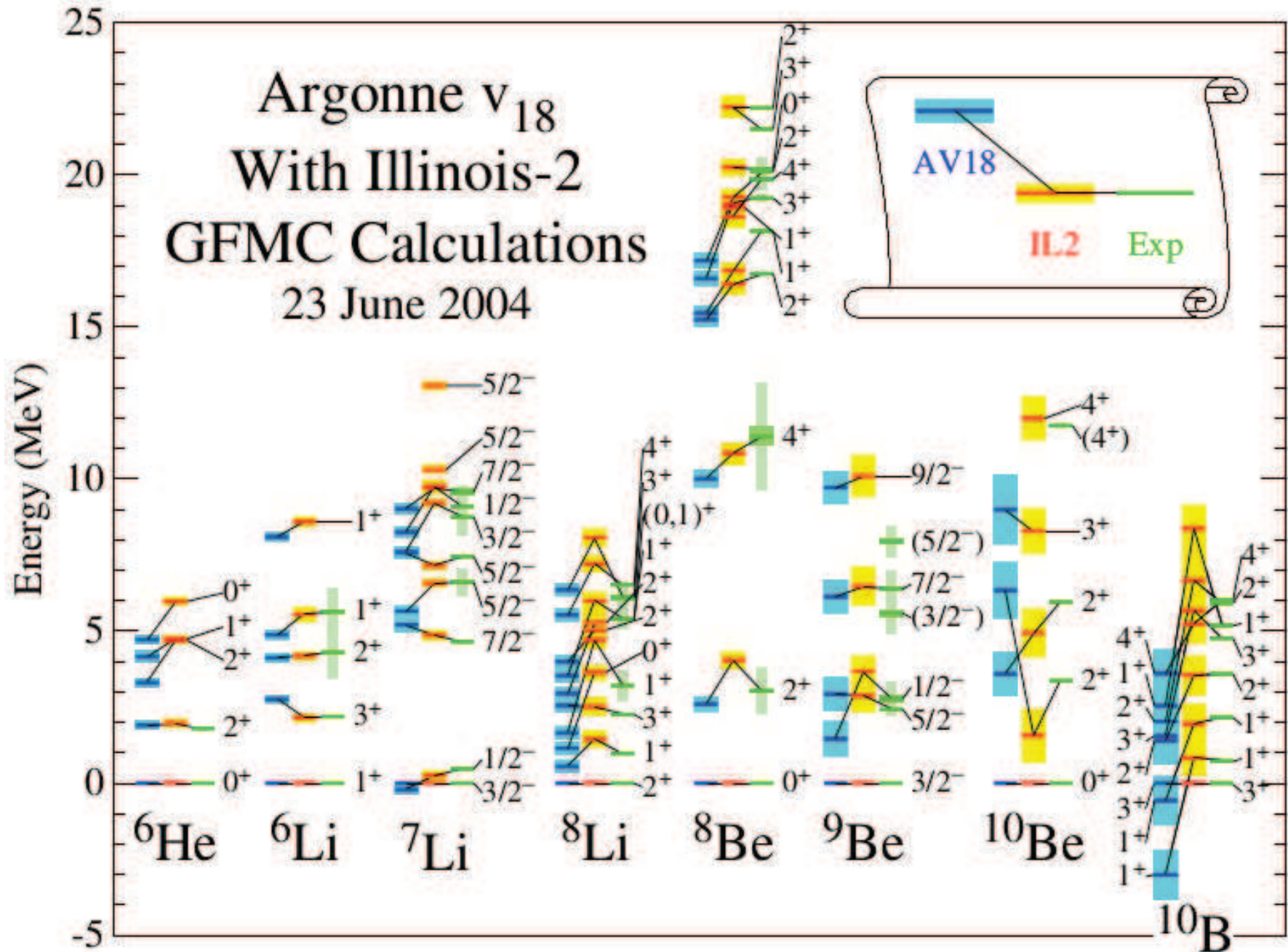
SNM saturation density is well reproduced



Nuclear Matter vs Pure Neutron Matter



Light Nuclei calculated with AV 18 + Illinois 2



The Experiment in which Tetraneutron was “Found”

PHYSICAL REVIEW C, VOLUME 65, 044006

Detection of neutron clusters

F. M. Marqués,^{1,*} M. Labiche,^{1,†} N. A. Orr,¹ J. C. Angélique,¹ L. Axelsson,² B. Benoit,³ U. C. Bergmann,⁴ M. J. G. Borge,⁵ W. N. Catford,⁶ S. P. G. Chappell,⁷ N. M. Clarke,⁸ G. Costa,⁹ N. Curtis,^{6,‡} A. D’Arrigo,³ E. de Góes Brennand,³ F. de Oliveira Santos,¹⁰ O. Doryvaux,⁹ G. Fazio,¹¹ M. Freer,^{8,‡} B. R. Fulton,^{8,§} G. Giardina,¹¹ S. Grévy,^{12,‡} D. Guillemaud-Mueller,¹² F. Hanappe,³ B. Heusch,⁹ B. Jonson,² C. Le Brun,¹³ S. Leenhardt,¹² M. Lewitowicz,¹⁰ M. J. López,^{10,**} K. Markenroth,² A. C. Mueller,¹² T. Nilsson,^{2,††} A. Ninane,^{2,‡‡} G. Nyman,¹ I. Piqueras,⁵ K. Riisager,⁴ M. G. Saint Laurent,^{10,§§} S. M. Singer,⁸ O. Sorlin,¹² and L. Stuttgé²

¹Laboratoire de Physique Corpusculaire, IN2P3-CNRS, ISMRA et Université de Caen, F-14050 Caen Cedex, France

²Experimentell Fysik, Chalmers Tekniska Högskolan, S-412 96 Göteborg, Sweden

³Université Libre de Bruxelles, CP 226, B-1050 Brussels, Belgium

⁴Institute for Fysik og Astronomi, Aarhus Universitet, DK-8000 Aarhus C, Denmark

⁵Instituto de Estructura de la Materia, CSIC, E-28006 Madrid, Spain

⁶Department of Physics, University of Surrey, Guildford, Surrey GU2 7XH, United Kingdom

⁷Department of Nuclear Physics, University of Oxford, Keele Road, Oxford OX1 3RH, United Kingdom

⁸School of Physics and Astronomy, University of Birmingham, Birmingham B15 2TT, United Kingdom

⁹Institut de Recherche Subatomique, IN2P3-CNRS, Université Louis Pasteur, BP 28, F-67037 Strasbourg Cedex, France

¹⁰GANIL, CEADSM-CNRS/IN2P3, BP 55027, F-14076 Caen Cedex, France

¹¹Dipartimento di Fisica, Università di Messina, Salita Spemme 31, I-98166 Messina, Italy

¹²Institut de Physique Nucléaire, IN2P3-CNRS, F-91406 Orsay Cedex, France

(Received 27 November 2001; published 1 April 2002)

A new approach to the production and detection of bound neutron clusters is presented. The technique is based on the breakup of beams of very neutron-rich nuclei and the subsequent detection of the recoiling proton in a liquid scintillator. The method has been tested in the breakup of intermediate energy (30–50 MeV/nucleon) ¹¹Li, ¹⁴Be, and ¹⁵B beams. *Some six events were observed that exhibit the characteristics of a multineutron cluster liberated in the breakup of ¹⁵Be, most probably in the channel ⁴He + ⁴n.* The various backgrounds that may mimic such a signal are discussed in detail.

DOI: 10.1103/PhysRevC.65.044006

PACS number(s): 21.45.+v, 25.10.+s, 21.10.Gv



nothing is known [4,5]. The discovery of such neutral systems as bound states would have far-reaching implications for many facets of nuclear physics. In the present paper, the production and detection of free neutron clusters is discussed.

The question as to whether neutral nuclei may exist has a long and checkered history that may be traced back to the early 1960s [5]. Forty years later, the only clear evidence in this respect is that the dineutron is particle unstable. Although ³n is the simplest multineutron candidate, the effects of pairing observed on the neutron drip line suggest that ^{4,6}n could exhibit bound states [6]. Concerning the tetraneutron, an upper limit on the binding energy of 3.1 MeV is provided by the particle stability of ⁶He, which does not decay into $\alpha + ^4n$. Furthermore, if ⁴n was bound by more than 1 MeV, $\alpha + ^4n$ would be the first particle threshold in ⁶He. As the breakup of ⁶He is dominated by the ⁶He channel [7], the tetraneutron, if bound, should be so by less than 1 MeV.

The majority of the calculations performed to date suggest that multineutron systems are unbound [4]. Interestingly, it was also found that subtle changes in the *N-N* potentials that do not affect the phase shift analysis may generate bound neutron clusters [5]. In addition to the complexity of such ab initio calculations, which include the uncertainties in many-body forces, the *n-n* interaction is the most poorly known *N-N* interaction, as demonstrated by the controversy regarding the determination of the scattering length a_{nn} [8]. The

Necessary stability condition for pairwise interacting matter

Theorem [Zhislin, Vugal'ter] Let $E(N)$ denote the ground state energy of N fermions (or bosons) that interact through the pair potential $v(\mathbf{r})$ satisfying the following condition

$$\int_{\mathbf{r}_1, \mathbf{r}_2 \in K} v(\mathbf{r}_1 - \mathbf{r}_2) d\mathbf{r}_1 d\mathbf{r}_2 < 0 \quad (1)$$

where K is a fixed arbitrary finite cube in \mathbb{R}^3 . Then

$$E(N) < -cN^2 \quad \text{for } N > N_0,$$

where $c, N_0 > 0$ are constants. Condition (1) can be improved

$$\int_{\mathbf{r}_1, \mathbf{r}_2 \in K_1} v(\mathbf{r}_1 - \mathbf{r}_2) d\mathbf{r}_1 d\mathbf{r}_2 + \int_{\substack{\mathbf{r}_1 \in K_1 \\ \mathbf{r}_2 \in K_2}} v(\mathbf{r}_1 - \mathbf{r}_2) d\mathbf{r}_1 d\mathbf{r}_2 < 0,$$

where $K_1 \cap K_2 = \emptyset$ are two disjoint cubes of equal size.

Sketch of the Proof

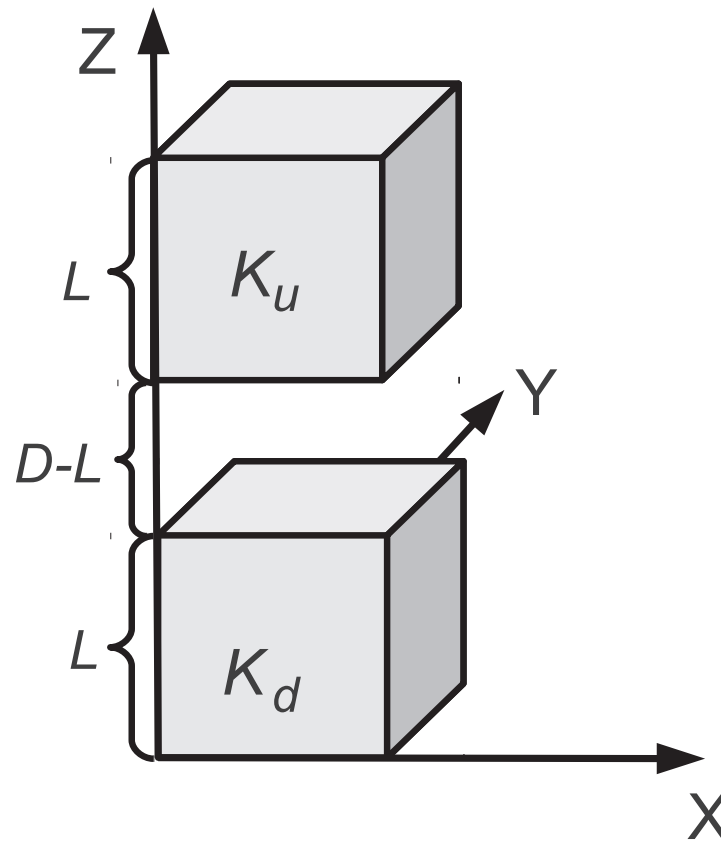


Figure: The neutrons are placed into two disjoint cubes K_u, K_d each with the side length L (subscripts u, d stand for “up” and “down” respectively). The upper cube is shifted by a distance D along the Z -axis with respect to the lower cube.

Sketch of the Proof

Consider $2N$ neutrons that are described by the following Hamiltonian

$$H = -\frac{\hbar^2}{2m} \sum_{i=1}^{2N} \Delta_{\mathbf{r}_i} + V_{2b} + V_{3b} = T + V_{2b} + V_{3b}.$$

The kinetic energy operator T includes the center of mass motion; m is the neutron mass and \mathbf{r}_i for $i = 1, \dots, 2N$ are neutrons' position vectors. The term $V_{2b} = \sum_{i < j} v_{ij}$ is the sum of two-nucleon interactions given by the Argonne V18 potential. The term V_{3b} is the three-body interaction, which can be one of the modern versions of Illinois three-nucleon interaction, namely Urbana IX or Illinois 7.

Construction of the Trial Function (1/2)

Each cube confines N neutrons, which form an excited state of the Fermi gas. The trial function depends on three parameters $L, D, \omega > 0$, where ω is an integer. For any $p = 1, 2, \dots$ and $x \in \mathbb{R}$ we set

$$\varphi_p(x) = (L/2)^{-1/2} \sin(2\pi p L^{-1} \omega x) \quad \text{if } x \in [0, L],$$

and $\varphi_p(x) = 0$ if $x \notin [0, L]$. Let us fix the an integer n in a way that makes the inequality $n^3 \leq N < (n+1)^3$ hold. For each $t = 1, \dots, N$ we choose a triple of positive integers $\{t_1, t_2, t_3\}$ so that $1 \leq t_1, t_2, t_3 \leq n+1$ and $\sum_{i=1}^3 |t_i - t'_i| \neq 0$ for $t \neq t'$. Using these triples we define the one particle states for $t = 1, \dots, N$ as follows

$$f_t(\mathbf{r}) := \varphi_{t_1}(r^x) \varphi_{t_2}(r^y) \varphi_{t_3}(r^z),$$

where r^x, r^y, r^z are the Cartesian components of the vector \mathbf{r} .

Construction of the Trial Function (2/2)

Let us set

$$\begin{aligned} \Psi_{\Pi}(\mathbf{r}_1, \dots, \mathbf{r}_{2N}) &:= f_1(\mathbf{r}_1) f_2(\mathbf{r}_2) \cdots f_N(\mathbf{r}_N) \\ &\times f_1(\mathbf{r}_{N+1} - \mathbf{D}) f_2(\mathbf{r}_{N+2} - \mathbf{D}) \cdots f_N(\mathbf{r}_{2N} - \mathbf{D}), \end{aligned}$$

where $\mathbf{D} := (0, 0, D)$ is a three-dimensional vector. We construct the trial function for $2N$ neutrons as

$$\tilde{\Psi}_A = \Psi_A(\mathbf{r}_1, \dots, \mathbf{r}_{2N}) |n \uparrow\rangle |n \uparrow\rangle \cdots |n \uparrow\rangle,$$

where the spatial part of the wave function is $\Psi_A = \sqrt{(2N)!} \mathcal{A} \Psi_{\Pi}$. Here \mathcal{A} is an antisymmetrizer on the permutation group for $2N$ particles \mathbb{S}_{2N} (only spatial coordinates are permuted).

Poof (continued)

By the variational principle

$$E(2N) \leq \langle \tilde{\Psi}_A | T | \tilde{\Psi}_A \rangle + \langle \tilde{\Psi}_A | V_{2b} | \tilde{\Psi}_A \rangle + \langle \tilde{\Psi}_A | V_{3b} | \tilde{\Psi}_A \rangle,$$

where $E(2N)$ is the ground state energy of $2N$ neutrons.

Contribution of kinetic energy is easy to compute

$$\langle \tilde{\Psi}_A | T | \tilde{\Psi}_A \rangle \leq \left(\frac{2\pi\omega\hbar}{\sqrt{mL}} \right)^2 \sum_{i=1}^{n+1} \sum_{j=1}^{n+1} \sum_{k=1}^{n+1} (i^2 + j^2 + k^2) = \mathcal{O}(N^{5/3})$$

Contribution of the 2-body interactions

$$\langle \tilde{\Psi}_A | V_{2b} | \tilde{\Psi}_A \rangle = \mathcal{O}(N^{8/3})$$

The power is different from 2 due the terms proportional to the square of the angular momentum.

3-body Term Contribution

$$\langle \tilde{\Psi}_A | V_{3b} | \tilde{\Psi}_A \rangle = QN^3 + \Upsilon(\omega)N^3$$

Let $W(\mathbf{r}_1, \mathbf{r}_2, \mathbf{r}_3)$ be the 3-body interaction potential. Then the constant Q is defined through

$$Q = \int_{\mathbf{r}_1, \mathbf{r}_2, \mathbf{r}_3 \in K_d} W(\mathbf{r}_1, \mathbf{r}_2, \mathbf{r}_3) d\mathbf{r}_1 d\mathbf{r}_2 d\mathbf{r}_3 \\ + \int_{\substack{\mathbf{r}_1, \mathbf{r}_2 \in K_u \\ \mathbf{r}_3 \in K_d}} W(\mathbf{r}_1, \mathbf{r}_2, \mathbf{r}_3) d\mathbf{r}_1 d\mathbf{r}_2 d\mathbf{r}_3$$

Due to form-factors the constant Q can be made negative by taking the small size of the cubes.

Behavior of the 3-body Potential

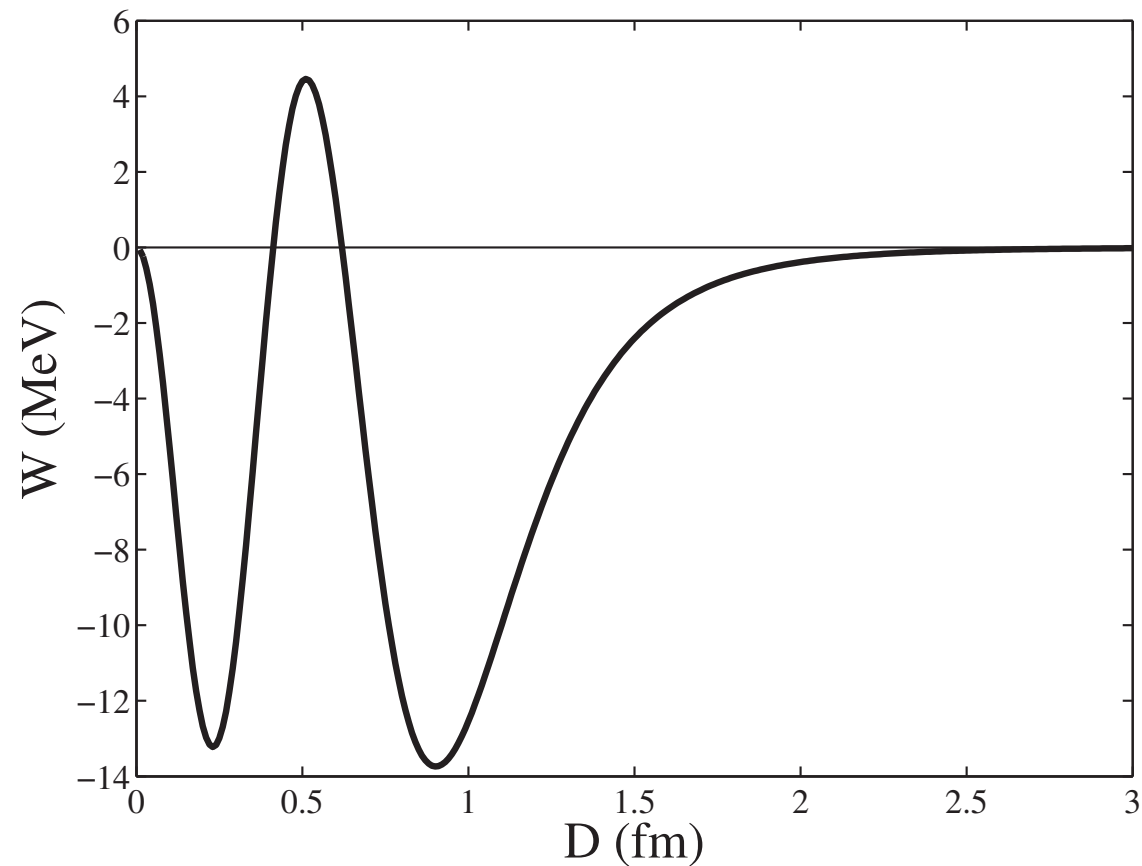


Figure: The plot of the function $W(0, 0, \mathbf{D})$ (where $\mathbf{D} \equiv (0, 0, D)$) versus parameter D . The plot shows that to ensure neutron matter collapse one can set $D = 1$ fm.

3-body Term Contribution

The constant Υ is defined through

$$\begin{aligned} \Upsilon(\omega) = \sup_{\mathbf{d} \in \mathcal{D}} & \left| \operatorname{Re} \int_0^L ds_1 \dots \int_0^L ds_9 W(\mathbf{s}) \right. \\ & \left. \times \exp(i2\pi L^{-1} \omega(\mathbf{d} \cdot \mathbf{s})) \right|, \end{aligned} \quad (8)$$

where \mathbf{d} is a non-zero vector with integer components. Note that $W(\mathbf{r}_1, \mathbf{r}_2, \mathbf{r}_3)$ is square-integrable in the cube, that is

$$\int_0^L ds_1 \dots \int_0^L ds_9 |W(\mathbf{s})|^2 < \infty. \quad (9)$$

By Bessel's inequality that $\Upsilon(\omega) \rightarrow 0$ for $\omega \rightarrow \infty$, since the integral in Eq. (8) is proportional to the Fourier coefficient of the function $W(\mathbf{s})$. Thus the total energy of $2N$ neutrons grows like $-QN^3$. **The matter cannot be formed!**

Behavior of the 3-body Potential

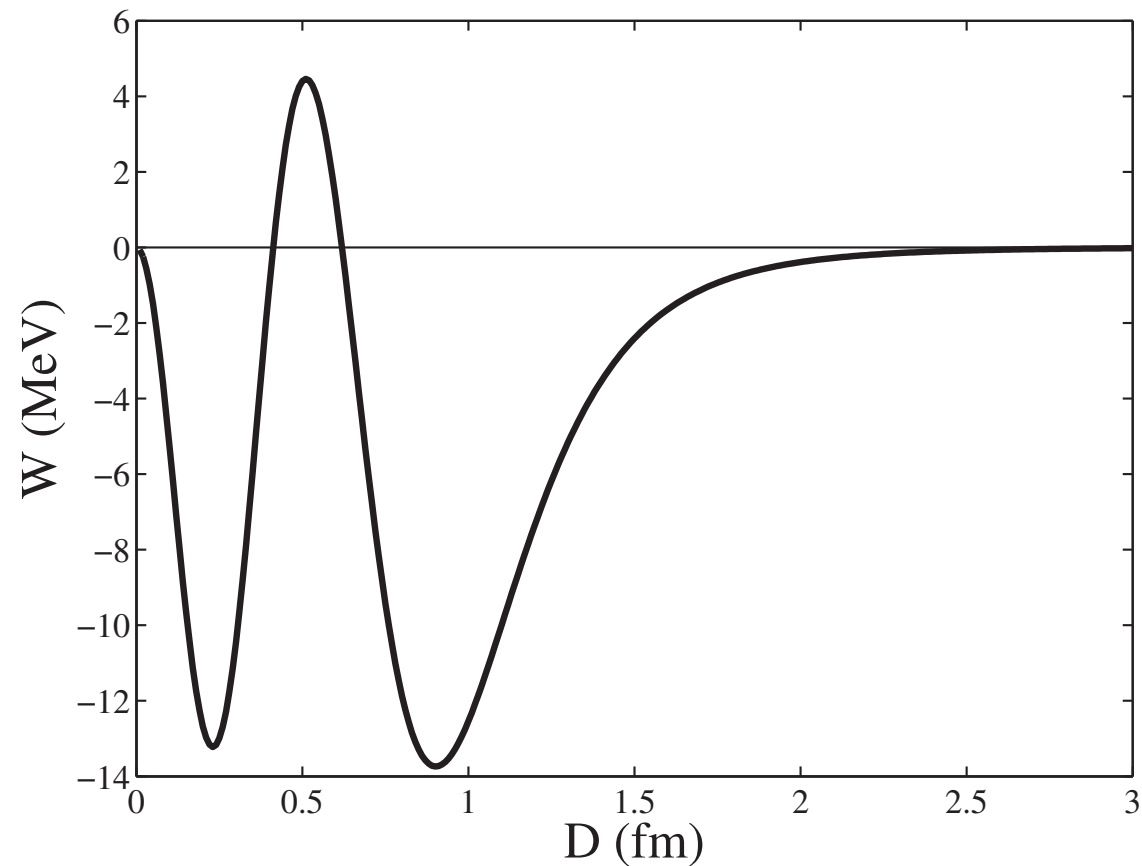


Figure: The plot of the function $W(0, 0, \mathbf{D})$ (where $\mathbf{D} \equiv (0, 0, D)$) versus parameter D . The plot shows that to ensure neutron matter collapse one can set $D = 1$ fm.

Collapsed Wave Function

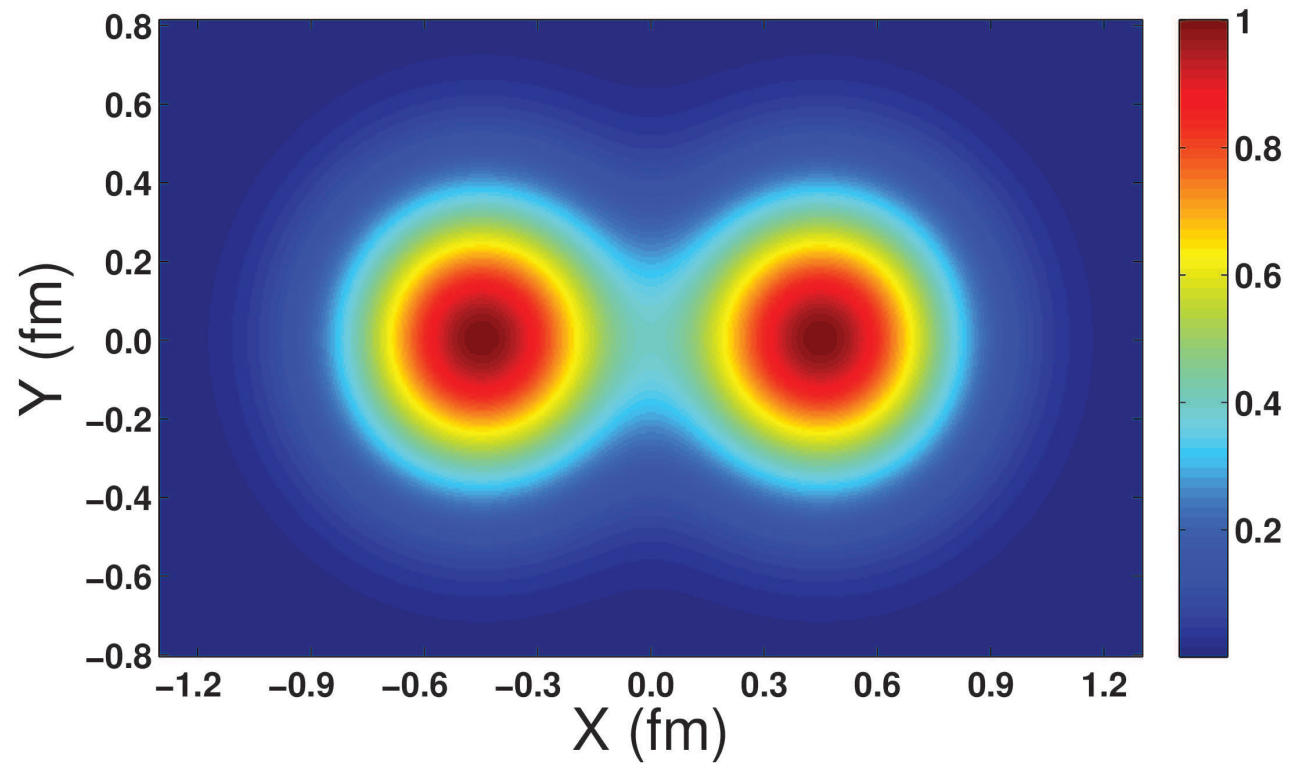


Figure: Schematic plot of density of 10000 neutrons.

Corrections are substantial

It is important to show that the required corrections of the 3-body interaction are substantial. Let us consider a hypothetical change in the Urbana IX interaction

$$\tilde{V}_{3b} = V_{3b} + V_{3NR},$$

where

$$V_{3NR}(\mathbf{r}_1, \mathbf{r}_2, \mathbf{r}_3) = U_C \mathcal{W}(r_{12}) \mathcal{W}(r_{13}) \mathcal{W}(r_{23}).$$

U_C is a constant and

$$\mathcal{W}(r) = \left[1 + \exp((r - R)c^{-1}) \right]^{-1}$$

with $R = 0.5$ fm and $c = 0.2$ fm.

Corrections are substantial

The necessary stability condition in the integral form reads

$$\begin{aligned} & \frac{1}{3}B_1 + B_2 + \frac{1}{3} \int_{\mathbf{r}_1, \mathbf{r}_2, \mathbf{r}_3 \in K_d} V_{3NR}(\mathbf{r}_1, \mathbf{r}_2, \mathbf{r}_3) d\mathbf{r}_1 d\mathbf{r}_2 d\mathbf{r}_3 \\ & + \int_{\mathbf{r}_1, \mathbf{r}_2, \mathbf{r}_3 \in K_d} V_{3NR}(\mathbf{r}_1, \mathbf{r}_2 + \mathbf{D}, \mathbf{r}_3 + \mathbf{D}) d\mathbf{r}_1 d\mathbf{r}_2 d\mathbf{r}_3 \geq 0, \end{aligned} \quad (10)$$

where

$$\begin{aligned} B_1 & := \int_{\mathbf{r}_1, \mathbf{r}_2, \mathbf{r}_3 \in K_d} W(\mathbf{r}_1, \mathbf{r}_2, \mathbf{r}_3) d\mathbf{r}_1 d\mathbf{r}_2 d\mathbf{r}_3 \\ B_2 & := \int_{\substack{\mathbf{r}_1 \in K_d \\ \mathbf{r}_2, \mathbf{r}_3 \in K_u}} W(\mathbf{r}_1, \mathbf{r}_2, \mathbf{r}_3) d\mathbf{r}_1 d\mathbf{r}_2 d\mathbf{r}_3 \end{aligned}$$

Inequality (10) should hold for all values of the constants $L, D > 0$ such that $D - L > 0$ (the cubes should remain disjoint). Let us set $D = 0.9$ fm so that $W(0, 0, \mathbf{D}) \simeq -13.7$ MeV and take $L \rightarrow 0$. Then $U_C > 51$ MeV.

Conclusions

- ▶ Neutron matter with AV18+UIX forces is unstable: the binding energy of N neutrons in the ground state $E(N)$ grows proportionally to N^3
- ▶ The problem is due to the force vanishing when 3 nucleons occupy the same site in space
- ▶ Old Urbana VI three-body force does not have that problem
- ▶ The matter can be quasistable, one has to calculate the potential barriers and probabilities for their penetration
- ▶ Primitive Minnesota and Volkov types of interaction predict bound multineutrons with growing density: the matter is unstable in this case as well since $|E(N)| \simeq N^2$.
- ▶ Rigorous mathematical methods provide useful insight into the structure of nuclear forces